Computing KPP front speeds in time-periodic cellular and chaotic flows using an efficient Lagrangian method

Junlong Lyu[a], Zhongjian Wang[b], Jack Xin[c], Zhiwen Zhang[a,*]

[a]*Department of Mathematics, The University of Hong Kong, Pokfulam Road, Hong Kong SAR, China.*
[b]*Department of Statistics, The University of Chicago, Chicago, IL 60637, USA.*
[c]*Department of Mathematics, University of California at Irvine, Irvine, CA 92697, USA.*

Abstract

In this paper, we study propagation speeds of reaction-diffusion-advection (RDA) fronts in time-periodic cellular and chaotic flows with Kolmogorov-Petrovsky-Piskunov (KPP) nonlinearity. The variational principle reduces the computation of KPP front speeds to a principal eigenvalue problem on a periodic domain of a linear advection-diffusion operator with space-time periodic coefficients. We develop efficient Lagrangian methods to compute the principal eigenvalue through the Feynman-Kac formula. By estimating the convergence rate of Feynman-Kac semigroups and the operator splitting methods for approximating the linear advection-diffusion solution operators, we obtain convergence analysis for the proposed numerical methods. Finally, we present numerical results to demonstrate the accuracy and efficiency of the proposed method in computing KPP front speeds in time-periodic cellular and chaotic flows, especially the time-dependent Arnold-Beltrami-Childress (ABC) flow and time-dependent Kolmogorov flow in three-dimensional space.

AMS subject classification: 35K57, 47D08, 65C35, 65L20, 65N25.

Keywords: KPP fronts; cellular and chaotic flows; Feynman-Kac semigroups; Lagrangian method; operator splitting; eigenvalue problems; convergence analysis.

1. Introduction

Front propagation in complex fluid flows arises in many scientific areas such as chemical kinetics, combustion, biology, transport in porous media, and industrial deposition processes (see [41] for a review). A fundamental problem is to analyze and compute large scale front speeds in complex flows. An extensively studied model problem is the reaction-diffusion-advection (RDA) equation with Kolmogorov-Petrovsky-Piskunov (KPP) nonlinearity [20]. To be specific, the KPP equation is

$$u_t = \kappa \Delta_{\mathbf{x}} u + (\mathbf{v} \cdot \nabla_{\mathbf{x}}) u + \tau^{-1} f(u), \quad t \in \mathbb{R}^+, \quad \mathbf{x} = (x_1, ..., x_d)^T \in \mathbb{R}^d, \tag{1}$$

*Corresponding author
Email addresses: u3005480@connect.hku.hk (Junlong Lyu), zhongjian@statistics.uchicago.edu (Zhongjian Wang), jxin@math.uci.edu (Jack Xin), zhangzw@hku.hk (Zhiwen Zhang)

where κ is diffusion constant, τ is time scale of reaction rate, $\mathbf{v}$ is an incompressible velocity field (its precise definition will be discussed later), u is the concentration of reactant or population, and the KPP reaction $f(u) = u(1-u)$ satisfying $f(u) \le uf'(0)$. In our analysis and numerical examples, we will keep τ and κ fixed, while change the magnitude of the velocity field $\mathbf{v}$, which equivalently means changing the Péclet number.

Since the pioneering work of Kolmogorov, Petrovsky and Piskunov [20] and Fisher [11] on traveling fronts of the reaction-diffusion equations, this field has gone through enormous growth and development. Reaction-diffusion front propagation in fluid flows has been an active research topic for decades; see e.g.[14, 22, 2, 29, 30, 27] and references therein. Significant amounts of mathematical analysis and numerical works in this direction have been accomplished when the streamlines of fluid flow are either well-structured (regular motion) or fully random (ergodic motion). Yet, the often encountered less studied case is when the streamlines consist of both regular and irregular motions, while neither one takes up the entire phase space, such as the chaotic Arnold-Beltrami-Childress (ABC) flow [8, 3] and Kolmogorov flows [13, 5].

In recent years, much progress has been made in finite element computation of the KPP front propagation in time-periodic cellular and chaotic flows based on a linearized corrector equation. If the velocity field $\mathbf{v} = \mathbf{v}(\mathbf{x})$ in the KPP equation (1) is time-independent, the minimal front speed in direction $\mathbf{e}$ is given by the variational formula [28]: $c^*(\mathbf{e}) = \inf_{\lambda>0} \mu(\lambda)/\lambda$, where $\mu(\lambda)$ is the principal eigenvalue of the elliptic operator, $\mathcal{A}_1^\lambda$, namely,

$$\mathcal{A}_1^\lambda \Phi \equiv \kappa \Delta_{\mathbf{x}} \Phi + (2\lambda \mathbf{e} + \mathbf{v}) \cdot \nabla_{\mathbf{x}} \Phi + \big(\kappa\lambda^2 + \lambda \mathbf{v} \cdot \mathbf{e} + \tau^{-1} f'(0)\big)\Phi = \mu(\lambda)\Phi. \tag{2}$$

In Eq.(2), $\Phi \in L^2(\mathbb{T}^d)$, $\mathbb{T} = \mathbb{R}/\mathbb{Z}$ is the one-dimensional torus, and $\mathbf{v}$ is period 1 in all direction $x_i, 1 \le i \le d$. Accurate estimation of $c^*(\mathbf{e})$ boils down to computing principal eigenvalue of the operator $\mathcal{A}_1^\lambda$ in (2). Adaptive finite element methods (FEM) were successfully applied to solve (2) in [36, 35]. If the velocity field $\mathbf{v} = \mathbf{v}(\mathbf{x}, t)$ in the KPP equation (1) is periodic in time t, then the variational formula $c^*(\mathbf{e}) = \inf_{\lambda>0} \mu(\lambda)/\lambda$ still holds [15, 28], where $\mu(\lambda)$ is the principal eigenvalue of the time-periodic parabolic operator, $\mathcal{A}_2^\lambda$, namely,

$$\mathcal{A}_2^\lambda \Phi \equiv \kappa \Delta_{\mathbf{x}} \Phi + (2\lambda \mathbf{e} + \mathbf{v}) \cdot \nabla_{\mathbf{x}} \Phi + \big(\kappa\lambda^2 + \lambda \mathbf{v} \cdot \mathbf{e} + \tau^{-1} f'(0)\big)\Phi - \Phi_t = \mu(\lambda)\Phi, \tag{3}$$

on the space-time domain $\mathbb{T}^d \times [0, T]$ (T is the period of $\mathbf{v}$ in t), subject to the same boundary condition in $\mathbf{x}$ as (1) and periodic in t. An edge-averaged FEM with algebraic multigrid acceleration was developed in [42] to study KPP front speeds in two-dimensional time-periodic cellular flows with chaotic streamlines. Adaptive FEM methods provide an efficient way to investigate the KPP front speeds in time-periodic cellular and chaotic flows. However, when the magnitude of velocity field, A, is large and/or the dimension of spatial variables is big, say $d = 3$, it is extremely expensive to compute KPP front speeds by using the FEM.

Recently, we have made progress in developing robust Lagrangian numerical schemes for computing effective diffusivities in chaotic and random flows [40, 39, 21]. This motivates us to develop efficient Lagrangian methods to compute KPP front propagation in time-periodic cellular and chaotic flows in this paper, especially in time-dependent flows in three-dimensional space.

In this paper, we first apply operator splitting methods to approximate the solution operator of the linear advection-diffusion operator (see Eq.(4)), which is a non-autonomous evolution equation and corresponding to the linearization of the KPP equation. Then, we develop Lagrangian numerical schemes to compute the KPP front propagation through the Feynman-Kac formula, which establishes a link between parabolic PDEs and SDEs. Directly approximation of the Feynman-Kac formula is unstable, since the main contribution to the expectation comes from sample paths that visit maximal points of the potential; see Eq.(7). Alternatively, we study a normalized version, i.e., the Feynman-Kac semigroup. Specifically, the principal eigenvalue of $\mathcal{A}_1^\lambda$ and $\mathcal{A}_2^\lambda$ can be obtained by studying the convergence of Feynman-Kac semigroups for SDEs associated with operators $\mathcal{A}_1^\lambda$ and $\mathcal{A}_2^\lambda$ [6, 10]. We approximate the evolution of probability measures by a particle system and use resampling technique to reduce the variance. Moreover, we estimate the approximation of semigroups associated with the solution operator of non-autonomous evolution equation and obtain a convergence analysis for our method in computing the KPP front speeds.

We point out that using Feynman-Kac semigroups to estimate the principal eigenvalue of differential operators has a long history. It was developed in large deviation theory, where Feynman-Kac semigroups were used to calculating cumulant generating functions [7]. They were also used in important practical applications, such as the diffusion Monte Carlo (DMC) method [12]. In the case when the flow is autonomous, [10] gave a rigorous proof of convergence and error analysis using a backward error analysis approach. When the flow becomes non-autonomous, their method cannot be directly applied. There are several novelties in our paper. Firstly, we analyze the solution operator by an operator splitting method and estimate the error in the L_2 operator norm. Secondly, we prove the convergence of estimating principal eigenvalues by the Feynman-Kac semigroups for non-autonomous periodic systems. Furthermore, we develop the N-interacting particle system (N-IPS) method to numerically calculate principal eigenvalues, where several important 3D chaotic flows are investigated.

Finally, we carry out numerical experiments to demonstrate the accuracy and efficiency of the proposed method in computing KPP front speeds for time-periodic cellular and chaotic flows. Most importantly, we aim to investigate the dependence of KPP front speeds on the chaos (disorder) and strengthen of the flows. For space-time-periodic shear flow, the speed $c^*(A)$ obeys a quadratic enhancement law: $c^*(A) = c_0(1 + \alpha A^2) + O(A^3)$, $A \ll 1$, where c_0 is the KPP front speed in homogeneous media ($A = 0$) and $\alpha > 0$ depends only on flow $\mathbf{v}$. The study for complicated flows, e.g. 3D flows remains largely open. At large A, the solution of the principal eigenvalue problem (2) develops internal layers, which brings essential difficulty for the FEM. We will study this issue in Section 4.3. Numerical results show that our Lagrangian method is still very efficient when the magnitude of velocity field A and computational cost linearly depends on the dimension d of spatial variables in the KPP equation (1). Thus, we are able to compute the KPP front speeds for time-dependent cellular and chaotic flows of physical interests, including the time-dependent ABC flow and the time-dependent Kolmogorov flow in three-dimensional space. To the best of our knowledge, our work appears to be the first one in the literature to develop numerical methods to compute

KPP front speeds for 3D time-dependent flows.

The rest of the paper is organized as follows. In Section 2, we propose Lagrangian methods in computing KPP front speeds in time-periodic cellular and chaotic flows (1). In Section 3, we estimate the approximation of semigroups associated with the solution operators of non-autonomous evolution equations and obtain the convergence analysis for our method. In Section 4, we present numerical results to demonstrate the accuracy and efficiency of our method. In addition, we investigate the dependence of KPP front speeds on the chaos (disorder) and strengthen in the flows, especially in 3D time-dependent chaotic flows. Concluding remarks are made in Section 5. Finally, we collect several fundamental results for abstract linear evolution equations by semigroup theory in the Appendix.

2. Efficient Lagrangian methods in computing KPP front speeds

2.1. Computing principal eigenvalue via the Feynman-Kac formula

In this section, we develop Lagrangian methods to compute KPP front propagation via the Feynman-Kac formula. We consider the linearized corrector equation of the KPP equation (1), where the velocity field $\mathbf{v}(\mathbf{x}, t)$ is space-time periodic, mean zero, and divergence-free. To compute the KPP front speed $c^*(\mathbf{e})$ along direction $\mathbf{e}$, let w solve a linearized equation parameterized by $\lambda > 0$:

$$w_t = \mathcal{A}w := \kappa\Delta w + (2\lambda\mathbf{e} + \mathbf{v}) \cdot \nabla_{\mathbf{x}} w + \big(\kappa\lambda^2 + \lambda\mathbf{v} \cdot \mathbf{e} + \tau^{-1} f'(0)\big)w, \tag{4}$$

with initial condition $w(\mathbf{x}, 0) = 1$. Then, the principal eigenvalue $\mu(\lambda)$ is given by

$$\mu(\lambda) = \lim_{t\to\infty} \frac{1}{t} \ln \int_\Omega w(\mathbf{x}, t) d\mathbf{x}. \tag{5}$$

The number $\mu(\lambda)$ is also the principal Lyapunov exponent of the parabolic equation (4), which is convex and superlinear in large λ [28, 42]. Finally, we compute the KPP front speed using the variational formula $c^*(\mathbf{e}) = \inf_{\lambda>0} \mu(\lambda)/\lambda$.

To design Lagrangian methods, we decompose the operator $\mathcal{A}$ in (4) into $\mathcal{A} = \mathcal{L} + \mathcal{C}$, where $\mathcal{L} := \kappa\Delta + (2\lambda\mathbf{e} + \mathbf{v}) \cdot \nabla_{\mathbf{x}}$ and $\mathcal{C} := c(\mathbf{x}, t) = \big(\kappa\lambda^2 + \lambda\mathbf{v} \cdot \mathbf{e} + \tau^{-1} f'(0)\big)$. To approximate the operator $\mathcal{L}$, we define a SDE system, $\mathbf{X}^{t,\mathbf{x}}$, which follows

$$d\mathbf{X}^{t,\mathbf{x}} = \mathbf{b}(\mathbf{X}^{t,\mathbf{x}}, t)dt + \sqrt{2\kappa} d\mathbf{w}(t), \quad \mathbf{X}^{0,\mathbf{x}} = \mathbf{x}, \tag{6}$$

where the drift term $\mathbf{b} = 2\lambda\mathbf{e} + \mathbf{v}$ is determined by the advection field in the operator $\mathcal{L}$ and $\mathbf{w}(s)$ is a d-dimensional Brownian motion. The principal eigenvalue $\mu(\lambda)$ of (4) can be represented via the Feynman-Kac formula as

$$\mu(\lambda) = \lim_{t\to\infty} \frac{1}{t} \ln \mathbb{E}\Big(\exp\big(\int_0^t c(\mathbf{X}^{s,\mathbf{x}}, s) ds\big)\Big), \tag{7}$$

where the expectation $\mathbb{E}[\cdot]$ is over randomness induced by $\mathbf{w}(s)$.

If we apply the formula (5) to compute the principal eigenvalue $\mu(\lambda)$, we need to solve a parabolic-type PDE (4) using numerical methods, such as FEM. When the magnitude of velocity field is large and/or the dimension of spatial variables d is big (say $d = 3$), the FEM becomes extremely expensive. The Feynman-Kac formula (7) provides an alternative strategy to design Lagrangian methods to compute the principal eigenvalue $\mu(\lambda)$, and thus allows us to compute the KPP front speeds. As we will demonstrate in Section 4, the proposed Lagrangian methods are still efficient for computing KPP front speeds in 3D time-dependent chaotic flows.

Remark 2.1. When the velocity field in the KPP equation (1) is time-independent, construction of the Lagrangian method for computing KPP front speeds is straightforward. We simply replace the drift term $\mathbf{b}$ in (6) and the potential c in (7) by their time-independent counterparts.

2.2. Feynman-Kac semigroups

Directly solving (6) by Monte Carlo method and using the Feynman-Kac formula (7) to compute the principal eigenvalue $\mu(\lambda)$ is unstable as the main contribution to $\mathbb{E}\Big(\exp\big(\int_0^t c(\mathbf{X}^{s,\mathbf{x}}, s)ds\big)\Big)$ comes from sample paths that visit maximal or minimal points of the potential function c, which leads to inaccurate or even divergent results.

Accurate principal eigenvalue $\mu(\lambda)$ can be obtained by studying the convergence of the Feynman-Kac semigroup associated with the SDE system (6) and the potential c. Specifically, let $\mathcal{P}(\mathbb{T}^d)$ denote the set of probability measures over $\mathbb{T}^d$ and $S = \mathcal{C}^\infty(\mathbb{T}^d)$. We define the evolution operator associated with the process $(\mathbf{X}^{t,\mathbf{x}})_{t\geq 0}$ in (6) as

$$(\nu)(P_t\phi) = \mathbb{E}_\nu[\phi(\mathbf{X}^{t,\mathbf{x}})], \quad \forall \nu \in \mathcal{P}(\mathbb{T}^d),\ \phi \in S. \tag{8}$$

Similarly, we define its weighted counterpart as

$$(\nu)(P_t^c\phi) = \mathbb{E}_\nu\big[\phi(\mathbf{X}^{t,\mathbf{x}})\exp\big(\int_0^t c(\mathbf{X}^{s,\mathbf{x}}, s)\big)ds\big], \quad \forall \nu \in \mathcal{P}(\mathbb{T}^d),\ \phi \in S. \tag{9}$$

In other words, infinitesimal generators of P_t and P_t^c are $\mathcal{L}$ and $\mathcal{A} = \mathcal{L} + \mathcal{C}$, respectively.

Equipped with the definitions of the evolution operators P_t and P_t^c, we can define the Feynman-Kac semigroup Φ_t^c as follows

$$\Phi_t^c(\nu)(\phi) := \frac{(\nu)(P_t^c\phi)}{(\nu)(P_t^c 1)} = \frac{\mathbb{E}_\nu\Big(\phi(\mathbf{X}^{t,\mathbf{x}})\exp\big(\int_0^t c(\mathbf{X}^{s,\mathbf{x}}, s)\big)ds\Big)}{\mathbb{E}_\nu\Big(\exp\big(\int_0^t c(\mathbf{X}^{s,\mathbf{x}}, s)\big)ds\Big)}. \tag{10}$$

One can easily verify that for all $\nu \in \mathcal{P}(\mathbb{T}^d)$ and t_1, $t_2 \in \mathbb{R}_+$, $\Phi_{t_1}^c(\Phi_{t_2}^c(\nu)) = \Phi_{t_1+t_2}^c(\nu)$. Thus, the family of maps $\{\Phi_t^c\}_{t\geq 0}$ is a measure-valued semigroup.

Notice that we use T to denote the period of velocity in time. Therefore, we consider the Feynman-Kac semigroup for $t = nT, n \in \mathbb{N}$. Namely, we consider $\Phi_{nT}^c = (\Phi_T^c)^n$.

Proposition 2.2. From Theorem 3.7 and Theorem 3.8, there exists $C > 0$ such that

$$\left|\Phi^c_{nT}(\nu)(\phi) - \int_\Omega \phi d\nu_c\right| \leq C||\phi|| \exp(-\delta_c nT), \quad \forall \nu \in \mathcal{P}(\mathbb{T}^d),\ \phi \in S. \tag{11}$$

The exponential-decay property stated above ensures us to obtain an invariant measure ν_c for Φ^c_T from any initial measure ν. From the definition of μ_c, we know $\Phi^c_T(\nu_c) = \nu_c$, which means that for any $\phi \in S$

$$\int_{\mathbb{T}^d} \phi d\nu_c = (\int_{\mathbb{T}^d} P^c_T 1 d\nu_c)^{-1} \int_{\mathbb{T}^d} P^c_T \phi d\nu_c. \tag{12}$$

In this way we see that the principal eigenvalue of P^c_T is just $\int_{\mathbb{T}^d} P^c_T 1 d\nu_c$.

2.3. Numerical discretization and resampling techniques

We use numerical methods to discretize the SDE (6). For instance, Euler-Maruyama scheme gives us

$$\boldsymbol{X}_{i+1} = \boldsymbol{X}_i + \mathbf{b}(\boldsymbol{X}_i, t_i)\Delta t + \sqrt{2\kappa\Delta t}\boldsymbol{\omega}_i, \tag{13}$$

where $t_i = i\Delta t$, $\Delta t = T/M$, so M is the number of time discretization interval for each period. $\{\boldsymbol{\omega}_i\}_{i=1}^\infty$ are i.i.d. d-dimensional standard Gaussian random variables. The numerical scheme (13) defines an evolution operator (also known as transition operator) $P_i^{\Delta t}$:

$$P_i^{\Delta t}\phi(\boldsymbol{x}) = \mathbb{E}(\phi(\boldsymbol{X}_{i+1})|\boldsymbol{X}_i = \boldsymbol{x}). \tag{14}$$

The evolution operator $P_i^{\Delta t}$ describes how the values of a given function evolve on average over one time step Δt. One can easily verify that

$$\left|\left|P_i^{\Delta t} - e^{\Delta t \mathcal{L}(t_i)}\right|\right|_{L^2} \leq C(\Delta t)^2, \tag{15}$$

where C is a positive constant [24]. Specially, when $\mathbf{b} = 0$, $P_{t_i}^{\Delta t} = e^{\Delta t \mathcal{L}(t_i)}$ for all i. Therefore, solving the SDE system (6) by the numerical scheme (13) provides a good approximation to the evolution operator $e^{\Delta t \mathcal{L}(t_i)}$, which plays an important role in the error estiamte of our Lagrangian methods in Section 3.

In addition, we can define the approximation operator for P^c_t in (9). For instance, if we choose the left-point rectangular integration, we obtain

$$(\nu)(P_i^{\Delta t} e^{\Delta t \mathcal{C}(t_i)}\phi) = \mathbb{E}\Big[\phi(\boldsymbol{X}_{i+1}) \exp\big(c(\boldsymbol{X}_{i+1}, t_i)\Delta t\big)\Big|\boldsymbol{X}_i \sim \nu\Big], \quad i = 1, 2, ..., M. \tag{16}$$

The time discretization for Feynman-Kac semigroup (10) reads:

$$\Phi_i^{\mathcal{C},\Delta t}(\nu)(\phi) = \frac{(\nu)(P_i^{\Delta t} e^{\Delta t \mathcal{C}(t_i)}\phi)}{(\nu)(P_i^{\Delta t} e^{\Delta t \mathcal{C}(t_i)} 1)}, \quad i = 0, 1, 2, ..., M-1. \tag{17}$$

It is difficult to obtain a closed-form solution to the evolution of probability measure in (17). Therefore, we propose to discretize the SDE system (6) by using numerical methods and approximate the evolution of probability measure in (17) by an N-interacting particle

system (N-IPS) [26]. Let us introduce the notation $\mathcal{K}^{\Delta t}=\mathcal{K}^{\Delta t,M-1}\mathcal{K}^{\Delta t,M-2}\cdots\mathcal{K}^{\Delta t,0}$, where $\mathcal{K}^{\Delta t,i}=P_i^{\Delta t}e^{\Delta t\mathcal{C}(t_i)}$, $M\Delta t=T$ in one time period, e.g. $[0,T]$. We denote

$$\Phi^{\mathcal{K}^{\Delta t,i}}(\nu)(\phi)=\frac{(\nu)(\mathcal{K}^{\Delta t,i}\phi)}{(\nu)(\mathcal{K}^{\Delta t,i}1)} \tag{18}$$

the Feynman-Kac semigroup associated with the operator $\mathcal{K}^{\Delta t,i}$. Then, according to Lemma 3.6, it satisfies

$$\Phi^{\mathcal{K}^{\Delta t}}=\prod_{i=0}^{M-1}\Phi^{\mathcal{K}^{\Delta t,i}}=\Phi^{\mathcal{K}^{\Delta t,0}}\Phi^{\mathcal{K}^{\Delta t,1}}\cdots\Phi^{\mathcal{K}^{\Delta t,M-1}}. \tag{19}$$

Suppose the Markov process $(\Theta,(\mathcal{F}_n)_{n\geq 0},(\xi^n)_{n\geq 0},\mathbb{P})$ is defined in the product space $(\mathbb{T}^d)^N$. We approximate any initial probability measure $\pi_0=\nu$ by

$$P(\boldsymbol{\xi}^0\in d\boldsymbol{z})=\prod_{p=1}^{N}\pi_0(dz^p), \tag{20}$$

and

$$P(\boldsymbol{\xi}^n\in d\boldsymbol{z}|\boldsymbol{\xi}^{n-1}=\boldsymbol{x})=\prod_{p=1}^{N}\Phi^{\mathcal{K}^{\Delta t}}(\frac{1}{N}\sum_{i=1}^{N}\delta_{x^i})(dz^p)=\prod_{p=1}^{N}(\prod_{i=0}^{M-1}\Phi^{\mathcal{K}^{\Delta t,i}})(\frac{1}{N}\sum_{i=1}^{N}\delta_{x^i})(dz^p), \tag{21}$$

where n denotes the iteration number in the evolution of probability measure by the Feynman-Kac semigroup (17).

From Eq.(20), we can figure out the evolution from $\boldsymbol{\xi}^{n-1}$ to $\boldsymbol{\xi}^n$. It will be divided into M small steps. Lets denote $\boldsymbol{\xi}_0^n=\boldsymbol{\xi}^n$ for all n. Within each iteration stage $n-1$, we evolve the particles from $t=0$ to $t=T$ by evolution operator $P_i^{\Delta t}$ and resampling techniques. Specifically, at $t=t_i$, $i=0,...,M-1$, we evolve the particles $\boldsymbol{\xi}_i^{n-1}$ by using the numerical scheme (13) and get $\widetilde{\boldsymbol{\xi}}_{i+1}^{n-1}$. That means

$$\widetilde{\xi}_{i+1}^{p,n-1}=\xi_i^{p,n-1}+\mathbf{b}(\xi_i^{p,n-1},t_i)\Delta t+\sqrt{2\kappa\Delta t}\boldsymbol{\omega}_i^{p,n-1},\quad p=1,2,...,N, \tag{22}$$

where $\boldsymbol{\omega}_i^{p,n-1}$ are i.i.d. d-dimensional standard Gaussian random variables.

Then, we resample the elements in $\widetilde{\boldsymbol{\xi}}_{i+1}^{n-1}$ according to the multinomial distribution with the weights

$$w_i^{j,n-1}=\frac{\exp\left(c(\widetilde{\xi}_i^{p,n-1},t_i)\Delta t\right)}{\sum_{p=1}^{N}\exp\left(c(\widetilde{\xi}_i^{p,n-1},t_i)\Delta t\right)},\quad p=1,...,N, \tag{23}$$

and obtain $\boldsymbol{\xi}_{i+1}^{n-1}$.

The evolution of N-IPS from $(n-1)T$ to nT can be represented as follows

$$\begin{aligned}&\boldsymbol{\xi}_0^{n-1}=(\xi_0^{1,n-1},\cdots,\xi_0^{N,n-1})\longrightarrow\boldsymbol{\xi}_1^{n-1}=(\xi_1^{1,n-1},\cdots,\xi_1^{N,n-1})\longrightarrow\\&\cdots\longrightarrow\boldsymbol{\xi}_M^{n-1}=(\xi_M^{1,n-1},\cdots,\xi_M^{N,n-1})=\boldsymbol{\xi}_0^{n}=(\xi_0^{1,n},\cdots,\xi_0^{N,n}).\end{aligned} \tag{24}$$

We know that the empirical distribution of the particles $\boldsymbol{\xi}_0^n$ will weakly converge to the distribution $\Phi_n^{\mathcal{K}^{\Delta t}}(\pi_0)$ as $N \to \infty$.

After obtaining the empirical distribution of the particles $\boldsymbol{\xi}_0^n$, we can compute the principal eigenvalues. At the iteration stage n, we first define the change of the mass as follows

$$e_{i,n}^N = N^{-1} \sum_{p=1}^{N} \exp(c(\widetilde{\xi}_i^{p,n-1}, t_i)\Delta t). \tag{25}$$

Then, we compute the approximation of the principal eigenvalue by

$$\mu_{\Delta t}^n(\lambda) = (M\Delta t)^{-1} \sum_{i=1}^{M} \log\Big(N^{-1} \sum_{p=1}^{N} \exp(c(\widetilde{\xi}_i^{p,n-1}, t_i)\Delta t)\Big). \tag{26}$$

Finally, we give the complete algorithm in Algorithm 1. The performance of our method will be demonstrated in Section 4.

Algorithm 1 Algorithm for computing the principal eigenvalues of parabolic equations

Input: velocity field $\mathbf{v}(\mathbf{x}, t)$, potential $c(\mathbf{x}, t)$, number of N-IPS system (i.e., N), N independent samples from initial distribution ν_0, iteration number n, time period T, and time step $\Delta t = T/M$.

1: Generates N i.i.d. ν_0-distributed random variables on $[0,1]^d$: $\boldsymbol{\xi}_0^1 = (\xi_0^{1,1}, \cdots, \xi_0^{N,1})$.
2: **for** $i = 1 : n$ **do**
3: **for** $j = 0 : M-1$ **do**
4: Generates standard normal variables ω_j^i and compute $\widetilde{\boldsymbol{\xi}}_{j+1}^{i-1}$ by (13).
5: Compute the pointwise value $\boldsymbol{S} = (e^{C^1}, \cdots, e^{C^N})$, where $C^j = c(\widetilde{\boldsymbol{\xi}}_j^{i-1}, j\Delta t)\Delta t$.
6: Compute weights $\boldsymbol{w} = (w^1, \cdots, w^N) = \boldsymbol{S}/\mathrm{SUM}(\boldsymbol{S})$ and $\mathbf{E}_{i,j} = \frac{1}{\Delta t}\log(\mathrm{mean}(\boldsymbol{S}))$.
7: Resample $\widetilde{\boldsymbol{\xi}}_{j+1}^{i-1}$ according to multinomial distribution with weight $\boldsymbol{w}$, and get $\boldsymbol{\xi}_{j+1}^{i-1}$.
8: **end for**
9: Compute $\mathbf{E}_i = M^{-1}\sum_{j=0}^{M-1}(\mathbf{E}_{i,j})$ and define $\boldsymbol{\xi}_M^{i-1} = \boldsymbol{\xi}_0^i$.
10: **end for**

Output: The approx invariant distribution $\Phi_n^{\mathcal{K}^{\Delta t}}(\nu)$-distributed variable $\boldsymbol{\xi}_n^0$ and approx eigenvalue $\widetilde{\lambda}_{n,\Delta t} = n^{-1}\sum_{i=1}^{n}\mathbf{E}_i$;

Remark 2.1. When the flow is time-independent, we can view it as a periodic flow with any given period T. The principal eigenvalue calculated by (5) will be the same with any $T > 0$. Hence the numerical schemes and the convergence analysis proposed in time-dependent flow can be applied by assigning $T = \Delta t$ and $M = 1$.

3. Convergence analysis of the Lagrangian method

In this section, we will prove the convergence of the Lagrangian method in computing KPP front speed. We divide the analysis into two parts. The first part studies the approximation of

the evolution of parabolic operators by using an operator splitting method. The second part studies the error estimate of the Lagrangian method in computing the principal eigenvalue of parabolic operators.

3.1. Approximation the evolution of parabolic operators

We first rewrite the linearized corrector equation of the KPP equation (4) into the following non-autonomous parabolic equation

$$w_t = \kappa\Delta_{\mathbf{x}} w + b(t,\mathbf{x})\cdot\nabla_{\mathbf{x}} w + c(t,\mathbf{x})w, \quad \mathbf{x} = (x_1,...,x_d)^T \in \mathbb{T}^d = [0,1]^d, \quad t\in[0,T], \quad (27)$$

where the initial condition $w(0,\mathbf{x}) = w_0$, $b(t,\mathbf{x}) = 2\lambda\mathbf{e} + \mathbf{v}$, $c(t,\mathbf{x}) = \kappa\lambda^2 + \lambda\mathbf{v}\cdot\mathbf{e} + \tau^{-1}f'(0)$, and T is final computational time. Since the velocity $\mathbf{v} = \mathbf{v}(t,\mathbf{x})$ is space-time periodic, so do $b(t,\mathbf{x})$ and $c(t,\mathbf{x})$. We assume the period of $b(t,\mathbf{x})$ and $c(t,\mathbf{x})$ is 1 in each dimension and they are smooth functions. For notational simplicity, we define

$$\mathcal{A}(t) = \mathcal{L}(t) + \mathcal{C}(t), \quad (28)$$

where $\mathcal{L}(t) := \kappa\Delta_{\mathbf{x}} + b(t,\mathbf{x})\cdot\nabla_{\mathbf{x}}$ and $\mathcal{C}(t) = c(t,\mathbf{x})$. As we have discussed in Section 2.2, the operator $\mathcal{A}(t)$ has a real isolated principal eigenvalue $\mu(\lambda)$. We aim to obtain error estimates of our Lagrangian method in approximating the principal eigenvalue $\mu(\lambda)$. To this end, we study the approximation the solution operator for the parabolic equation (27) by using an operator splitting method.

We define the solution operator $\mathcal{U}(t,s)$ corresponding to the parabolic equation (27), which satisfies the following properties:

1. $\mathcal{U}(s,s) = Id$, for any $s \geq 0$;
2. $\mathcal{U}(t,r)\circ\mathcal{U}(r,s) = \mathcal{U}(t,s)$, for any $t \geq r \geq s \geq 0$;
3. $\frac{d}{dt}\mathcal{U}(t,s)w_0 = \mathcal{A}(t)\mathcal{U}(t,s)w_0$, for any $t \geq s \geq 0, w_0 \in L^2([0,1]^d)$.

The solution operator $\mathcal{U}(t,s)$ enables us to study the evolution of parabolic operator in (27), e.g., the principal eigenvalue of $\mathcal{U}(T,0)$ gives the principal eigenvalue of the parabolic operator $\mathcal{A}(t)$. It has been proven that the principal eigenvalue of $\mathcal{U}(T,0)$ exists and is real [15]. It is difficult to obtain a closed-form for the solution operator $\mathcal{U}(T,0)$. Therefore, we approximate the solution operator $\mathcal{U}(T,0)$ by using an operator splitting method.

We set $t_i = i\Delta t$ with $\Delta t = \frac{T}{M}$ and consider the following parabolic equation with freezing time coefficients.

$$w_t = \kappa\Delta_{\mathbf{x}} w + b(t_i,\mathbf{x})\cdot\nabla_{\mathbf{x}} w + c(t_i,\mathbf{x})w, \quad t_i < t \leq t_{i+1}, \quad i \geq 0, \quad (29)$$

The corresponding solution operator can be formally represented as

$$w(t) = e^{(t-t_i)(\mathcal{L}+\mathcal{C})(t_i)} \prod_{k=0}^{i-1} e^{\Delta t(\mathcal{L}+\mathcal{C})(t_k)} w_0, \quad t_i \leq t < t_{i+1}, \quad (30)$$

Furthermore, we can apply the first-order Lie-Trotter operator splitting method to approximate the solution operator defined in (30) and obtain

$$w(t) = e^{(t-t_i)\mathcal{L}(t_i)} e^{(t-t_i)\mathcal{C}(t_i)} \prod_{k=0}^{i-1} e^{\Delta t \mathcal{L}(t_j)} e^{\Delta t \mathcal{C}(t_j)} w_0, \quad t_i \le t < t_{i+1}, \tag{31}$$

We will prove the solution operator $\prod_{j=0}^{M-1} e^{\Delta t \mathcal{L}(t_j)} e^{\Delta t \mathcal{C}(t_j)}$ obtained by the Lie-Trotter operator splitting method converges to the solution operator $\mathcal{U}(T,0)$ in certain operator norm as Δt approaches zero. As a consequence of this convergence result, we can further prove the convergence of the principal eigenvalue associated with these two solution operators.

To make our paper self-contained, we collect several fundamental results for abstract linear evolution equations by semigroup theory in Appendix A. We begin with following lemma, which is as a special case of Theorem 1 in [37].

Lemma 3.1. Let t be fixed. If $b(t,\mathbf{x})$ and $c(t,\mathbf{x})$ are smooth and bounded, then the operator $\mathcal{A}(t)$ defined in (28) is a strongly elliptic operator on $\mathbb{T}^d$. Moreover, $\mathcal{A}(t)$ generates an analytic semigroup $e^{\cdot \mathcal{A}(t)}$ in $L^p(\mathcal{D})$, for all $1 \le p \le \infty$.

We will prove that, in our non-autonomous parabolic equation setting, the assumptions made in Appendix A are all satisfied, so we can obtain the error of the operator splitting method in approximation the non-autonomous parabolic operator.

We first prove the operator $\mathcal{A}$ defined in (28) satisfies a Hölder continuous condition.

Lemma 3.2. Suppose $b(t,\mathbf{x})$ and $c(t,\mathbf{x})$ in the operator $\mathcal{A}(t)$ are bounded, smooth and periodic in each component of $\mathbf{x}$, and uniformly Hölder continuous in t, i.e., for any $t, s \in \mathbb{R}^+$,

$$\big|\big|b(t,\mathbf{x}) - b(s,\mathbf{x})\big|\big| \le C_1|t-s|^\beta, \quad \big|c(t,\mathbf{x}) - c(s,\mathbf{x})\big| \le C_1|t-s|^\beta, \tag{32}$$

for some positive C_1 and β. Let $v \in \mathcal{D}(\mathcal{A}(\cdot)) = H^2(\mathbb{T}^d)$ is periodic. Then, for any $0 < s \le \tau$, there exists $\gamma_1 > 0$, such that

$$\big|\big|\mathcal{A}(\tau)v - \mathcal{A}(s)v\big|\big|_{L^2} \le C_2(\tau-s)^\beta \big|\big|(\mathcal{A}(t)-\gamma_1)v\big|\big|_{L^2}^{1/2} \big|\big|v\big|\big|_{L^2}^{1/2}, \tag{33}$$

for any $t \in \mathbb{R}^+$. Specifically, if $b(t,\mathbf{x}) = 0$, then

$$\big|\big|\mathcal{A}(\tau)v - \mathcal{A}(s)v\big|\big|_{L^2} \le C_3(\tau-s)^\beta \big|\big|v\big|\big|_{L^2}. \tag{34}$$

Proof. We first consider the case when $b(t,\mathbf{x}) \neq 0$. By using the uniformly Hölder continuous conditions for $b(t,\mathbf{x})$ and $c(t,\mathbf{x})$, we have

$$\begin{aligned} \big|\big|\mathcal{A}(\tau)v - \mathcal{A}(s)v\big|\big|_{L^2} =& \big|\big|(b(\tau,\mathbf{x}) - b(s,\mathbf{x}))\cdot\nabla_{\mathbf{x}} v + (c(\tau,\mathbf{x}) - c(s,\mathbf{x}))v\big|\big|_{L^2} \\ \le& C_1(t-s)^\beta(||\nabla_{\mathbf{x}} v||_{L^2} + ||v||_{L^2}). \end{aligned} \tag{35}$$

For the operator $\mathcal{A}(t)$, we claim that there exists $\gamma_1 > 0$ such that,

$$\big|\big|(\mathcal{A}(t)-\gamma_1)v\big|\big|_{L^2} > C(\kappa,b,c)\big(||\Delta_{\mathbf{x}} v||_{L^2} + ||v||_{L^2}\big), \quad \forall v \in \mathcal{D}(\mathcal{A}(\cdot)), \tag{36}$$

where the constant $C(\kappa, b, c)$ depends on κ, $b(t, \mathbf{x})$ and $c(t, \mathbf{x})$.

We prove the statement in (36) before move to the main results. Let $c_{\gamma_1} = c - \gamma_1$ and assume $\big|\big|b(t, \mathbf{x})\big|\big| \leq M_1$, $|c(t, \mathbf{x})| \leq M_2$, $\big|\big|\nabla_{\mathbf{x}} c(t, \mathbf{x})\big|\big| \leq M_3$. We know that

$$\begin{aligned}\big|\big|(\mathcal{A}(t) - \gamma_1)v\big|\big|_{L^2} &= \big|\big|(\kappa\Delta_{\mathbf{x}} + b(t, \mathbf{x}) \cdot \nabla_{\mathbf{x}} + c_{\gamma_1}(t, \mathbf{x}))v\big|\big|_{L^2} \\ &\geq \big|\big|(\kappa\Delta_{\mathbf{x}} + c_{\gamma_1}(t, \mathbf{x}))v\big|\big|_{L^2} - \big|\big|b(t, \mathbf{x}) \cdot \nabla_{\mathbf{x}} v\big|\big|_{L^2}. \end{aligned} \tag{37}$$

For the term $\big|\big|(\kappa\Delta_{\mathbf{x}} + c_{\gamma_1}(t, \mathbf{x}))v\big|\big|_{L^2}$, the periodic condition of v implies that

$$\begin{aligned}&\big|\big|(\kappa\Delta_{\mathbf{x}} + c_{\gamma_1}(t, \mathbf{x}))v\big|\big|_{L^2}^2 \\ =&||\kappa\Delta_{\mathbf{x}} v||_{L^2}^2 + \big|\big|c_{\gamma_1}(t, \mathbf{x})v\big|\big|_{L^2}^2 - 2\langle\kappa\nabla_{\mathbf{x}} v, c_{\gamma_1}(t, \mathbf{x})\nabla_{\mathbf{x}} v\rangle_{L^2} - 2\langle\kappa\nabla_{\mathbf{x}} v, v\nabla_{\mathbf{x}} c(t, \mathbf{x})\rangle_{L^2} \end{aligned} \tag{38}$$

Notice that if we choose $\gamma_1 = \frac{2M_1^2}{\kappa} + M_2$, then we obtain

$$-2\langle\kappa\nabla_{\mathbf{x}} v, c_{\gamma_1}(t, \mathbf{x})\nabla_{\mathbf{x}} v\rangle_{L^2} \geq 4\kappa(\gamma_1 - M_2)||\nabla_{\mathbf{x}} v||_{L^2} \geq 4\big|\big|b(t, \mathbf{x}) \cdot \nabla_{\mathbf{x}} v\big|\big|_{L^2}. \tag{39}$$

In addition, we have

$$2\langle\kappa\nabla_{\mathbf{x}} v, v\nabla_{\mathbf{x}} c(t, \mathbf{x})\rangle_{L^2} \leq 2\kappa M_3||\nabla_{\mathbf{x}} v||_{L^2}||v||_{L^2} \leq 2\kappa M_3 C||\Delta_{\mathbf{x}} v||_{L^2}^{\frac{1}{2}}||v||_{L^2}^{\frac{3}{2}}. \tag{40}$$

Here, we use the fact that $||\nabla_{\mathbf{x}} v||_{L^2} \leq C||\Delta_{\mathbf{x}} v||_{L^2}^{\frac{1}{2}}||v||_{L^2}^{\frac{1}{2}}$, which is the moment inequality in interpolation theory; see Theorem 5.34 of [9]. If we take γ_1 large enough such that $4(\frac{\gamma_1 - M_2}{3})^{\frac{3}{4}}\kappa^{\frac{1}{4}} \geq 2\kappa M_3 C$, we get that

$$||\kappa\Delta_{\mathbf{x}} v||_{L^2}^2 + \big|\big|c_{\gamma_1}(t, \mathbf{x})v\big|\big|_{L^2}^2 \geq 2\kappa M_3 C||\Delta_{\mathbf{x}} v||_{L^2}^{\frac{1}{2}}||v||_{L^2}^{\frac{3}{2}} \geq 2\langle\kappa\nabla_{\mathbf{x}} v, v\nabla_{\mathbf{x}} c(t, \mathbf{x})\rangle_{L^2}. \tag{41}$$

Substititing the estiamtes (39)-(41) into (38), we obtain

$$\big|\big|(\kappa\Delta_{\mathbf{x}} + c_{\gamma_1}(t, \mathbf{x}))v\big|\big|_{L^2} \geq 2\big|\big|b(t, \mathbf{x}) \cdot \nabla_{\mathbf{x}} v\big|\big|_{L^2}. \tag{42}$$

Thus, from (37) we get that

$$\big|\big|(\mathcal{A}(t) - \gamma_1)v\big|\big|_{L^2} \geq \frac{1}{2}\big|\big|(\kappa\Delta_{\mathbf{x}} + c_{\gamma_1}(t, \mathbf{x}))v\big|\big|_{L^2}. \tag{43}$$

Using the same argument, we can prove that for γ_1 large enough,

$$\big|\big|(\kappa\Delta_{\mathbf{x}} + c_{\gamma_1}(t, \mathbf{x}))v\big|\big|_{L^2} \geq \hat{C}(||\Delta_{\mathbf{x}} v||_{L^2} + ||v||_{L^2}). \tag{44}$$

Finally, using the moment inequality we prove the statement in (33).

The case when $b(t, \mathbf{x}) = 0$ is simple since we have

$$\big|\big|\mathcal{A}(\tau)v - \mathcal{A}(s)v\big|\big|_{L^2} = \big|\big|(c(\tau, \mathbf{x}) - c(s, \mathbf{x}))v\big|\big|_{L^2} \leq C_3(t - s)^{\beta}||v||_{L^2}. \tag{45}$$

□

We then verify the operators $\mathcal{L}(t)$ and $\mathcal{C}(t)$ defined in (28) satisfy the assumption Appendix A.11. Given $\tau \geq 0$, we assume the bounded conditions as follows

$$||e^{\tau\mathcal{L}(t)}||_{L^2} \leq 1, \quad ||e^{\tau\mathcal{C}(t)}||_{L^2} \leq 1, \quad ||e^{\tau(\mathcal{L}(t)+\mathcal{C}(t))}||_{L^2} \leq 1. \tag{46}$$

Lemma 3.3. Suppose $b(t,\mathbf{x})$ and $c(t,\mathbf{x})$ in the operator $\mathcal{A}$ satisfy the same assumption as that in Lemma 3.2. Then, there exists $\gamma_2 > 0$ such that, for any periodic $v \in L^2(\mathbb{T}^d)$, commutator of $\mathcal{L}$ and $\mathcal{C}$ acting on v follows,

$$\big|\big|[\mathcal{L}(t),\mathcal{C}(t)]v\big|\big|_{L^2} \leq C_1\big|\big|(\mathcal{L}(t)-\gamma_2)v\big|\big|_{L^2}^{\frac{1}{2}}||v||_{L^2}^{\frac{1}{2}}, \quad \forall t \geq 0. \tag{47}$$

Proof. We first observe that, for any v periodic in $L^2(\mathbb{T}^d)$,

$$\begin{aligned}
&\big|\big|[\mathcal{L}(t),\mathcal{C}(t)]v\big|\big|_{L^2} = \big|\big|\mathcal{L}(t)(\mathcal{C}(t)v) - \mathcal{C}(t)(\mathcal{L}(t)v)\big|\big|_{L^2},\\
=&\big|\big|\big(\kappa\Delta_{\mathbf{x}}c(t,\mathbf{x}) + b(t,\mathbf{x})\cdot\nabla_{\mathbf{x}}c(t,\mathbf{x})\big)v + 2\kappa\nabla_{\mathbf{x}}c(t,\mathbf{x})\cdot\nabla v\big|\big|_{L^2},\\
\leq&(\kappa M_4 + M_1M_3)||v||_{L^2} + 2\kappa M_3||\nabla_{\mathbf{x}}v||_{L^2},
\end{aligned} \tag{48}$$

where $||b(t,\mathbf{x})|| \leq M_1$, $||\nabla_{\mathbf{x}}c(t,\mathbf{x})|| \leq M_3$, and $|\Delta_{\mathbf{x}}c(t,\mathbf{x})| \leq M_4$.

Following the same procedure as in the proof of Lemma 3.2, we have

$$\big|\big|(\mathcal{L}(t)-\gamma_1)v\big|\big|_{L^2} \geq C(\kappa,b)(||\Delta_{\mathbf{x}}v||_{L^2} + ||v||_{L^2}). \tag{49}$$

Using the fact that $||\nabla_{\mathbf{x}}v||_{L^2} \leq C||\Delta_{\mathbf{x}}v||_{L^2}^{\frac{1}{2}}||v||_{L^2}^{\frac{1}{2}}$, we prove finally the assertion in (47). □

Remark 3.1. If the bounded conditions (46) for $\mathcal{L}(t)$ and $\mathcal{C}(t)$ do not hold, we can shift the operators by a constant so that the shifted operators satisfy the bounded condition. Shift the operator by a constant will not affect the commutator in (47).

Now we are in the position to present the main result in approximating the solution operator $\mathcal{U}(t,s)$ for the parabolic equation (27).

Theorem 3.4. The solution operator (30) has the following error in approximating the solution operator $\mathcal{U}(T,0)$ in L^2 operator norm

$$||\mathcal{U}(T,0) - \prod_{k=0}^{M-1} e^{\Delta t\mathcal{A}(k\Delta t)}||_{L^2(\mathbb{T}^d)} \leq C_1(T)(\Delta t)^{\beta-\frac{1}{2}}, \tag{50}$$

where $T > 0$, M is an integer, and $\Delta t = \frac{T}{M}$. In addition, the Lie-Trotter operator splitting method has the following error in approximaing the solution operator (30)

$$\Big|\Big| \prod_{k=0}^{M-1} e^{\Delta t\mathcal{A}(k\Delta t)} - \prod_{k=0}^{M-1} e^{\Delta t\mathcal{L}(k\Delta t)}e^{\Delta t\mathcal{C}(k\Delta t)}\Big|\Big|_{L^2(\mathbb{T}^d)} \leq C_2(T)(\Delta t)^{\frac{1}{2}}. \tag{51}$$

Proof. We take $\gamma = \max(\gamma_1, \gamma_2)$, where γ_1 and γ_2 are defined in Lemma 3.2 and Lemma 3.3 respectively. Let $\mathcal{U}_\gamma(t,s) = e^{-\gamma(t-s)}\mathcal{U}(t,s)$ corresponding the solution operator to the parabolic equation (27) with $\mathcal{A}_\gamma(t) = \mathcal{A}(t) - \gamma$, $\mathcal{L}_\gamma(t) = \mathcal{L}(t) - \gamma$ Then, we have

$$\mathcal{U}(T,0) - \prod_{k=0}^{M-1} e^{\Delta t \mathcal{A}(k\Delta t)} = e^{\gamma T}(U_\gamma(T,0) - \prod_{k=0}^{M-1} e^{\Delta t A_\gamma(k\Delta t)}) \tag{52}$$

The statement in (50) is proved accoeding to Theorem Appendix A.9.

For the Lie-Trotter operator splitting method, we know that

$$\prod_{k=0}^{M-1} e^{\Delta t \mathcal{A}(k\Delta t)} - \prod_{k=0}^{M-1} e^{\Delta t \mathcal{L}(k\Delta t)} e^{h\mathcal{C}(k\Delta t)} = e^{\gamma T}(\prod_{k=0}^{M-1} e^{\Delta t \mathcal{A}_\gamma(k\Delta t)} - \prod_{k=0}^{M-1} e^{\Delta t L_\gamma(k\Delta t)} e^{\Delta t M(k\Delta t)}) \tag{53}$$

Now according to the Lemma 3.2 and 3.3, $\mathcal{A}_\gamma(k\Delta t) = \mathcal{L}_\gamma(k\Delta t) + \mathcal{C}(k\Delta t)$ and $\mathcal{L}_\gamma$ and $\mathcal{C}$ satisfy the assumptions Appendix A.10 and Appendix A.11. Thus, applying Theorem Appendix A.12 and Theorem Appendix A.13, we can prove the estimate (51). □

The convergence of $\mathcal{K}^{\Delta t}$ in the operator norm $\mathcal{L}(L^2, H^1)$ has been proved in [1]. In Theorem 3.4 we obtain the convergence of $\mathcal{K}^{\Delta t}$ in the operator norm $\mathcal{L}(L^2)$. Finally, we can obtain the error estimate for the principal eigenvalue.

Theorem 3.5. Let $e^{\mu(\lambda)T}$ and $e^{\mu_{\Delta t}(\lambda)T}$ denote the principal eigenvalue of the solution operator $\mathcal{U}(T,0)$ and the approximated solution operator $\prod_{k=0}^{M-1} e^{\Delta t \mathcal{L}(k\Delta t)} e^{\Delta t \mathcal{C}(k\Delta t)}$, respectively. Then, we have the error estimate as follows:

$$\left| e^{\mu(\lambda)T} - e^{\mu_{\Delta t}(\lambda)T} \right| \leq C_1(T)(\Delta t)^{\beta - \frac{1}{2}} + C_2(T)(\Delta t)^{\frac{1}{2}}. \tag{54}$$

Hence, $|\mu(\lambda) - \mu_{\Delta t}(\lambda)| = O((\Delta t)^{\min(\beta - \frac{1}{2}, \frac{1}{2})})$.

Proof. According to the standard spectral theorem [19], the principal eigenvalue $e^{\mu(\lambda)}$ for the solution operator $\mathcal{U}(T,0)$ and the principal eigenvalue $e^{\mu_{\Delta t}(\lambda)}$ for the approximated solution operator $\prod_{k=0}^{M-1} e^{\Delta t \mathcal{L}(k\Delta t)} e^{\Delta t \mathcal{C}(k\Delta t)}$ satisfy

$$\left| e^{\mu(\lambda)T} - e^{\mu_{\Delta t}(\lambda)T} \right| \leq C_3 \left|\left| U(T,0) - \prod_{k=0}^{N-1} e^{\Delta t \mathcal{L}(k\Delta t)} e^{\Delta t \mathcal{C}(k\Delta t)} \right|\right|_{L^2(\mathbb{T}^d)}. \tag{55}$$

By using triangle inequality for the right hand side of (55) and the estimated results from Theorem 3.4, we can get the error estimate (54). □

If $b(t, \mathbf{x})$ and $c(t, \mathbf{x})$ in the operator $\mathcal{A}$ are uniformly Lipschitz, then the error of the principal eigenvalue obtained by the Lie-Trotter operator splitting method is $O((\Delta t)^{\frac{1}{2}})$.

3.2. Analysis of the Lagrangian method

We consider the Feynman-Kac semigroup $\Phi^{\mathcal{A}}$ associated with an arbitary operaor $\mathcal{A}$. The action of the Feynman-Kac semigroup $\Phi^{\mathcal{A}}$ on a probability measure ν is defined by

$$\Phi^{\mathcal{A}}(\nu)(\phi) = \frac{(\nu)(\mathcal{A}\phi)}{(\nu)(\mathcal{A}1)}, \quad \forall \phi \in L^2(\mathbb{T}^d). \tag{56}$$

Moreover, we denote $\Phi_n^{\mathcal{A}} = (\Phi^{\mathcal{A}})^n$. The Feynman-Kac semigroup operation satisfies the following property.

Lemma 3.6. For any operaors $\mathcal{A}$, $\mathcal{B}$ in $\mathcal{L}(L^2(\mathbb{T}^d))$, $\Phi^{\mathcal{A}\mathcal{B}} = \Phi^{\mathcal{B}}\Phi^{\mathcal{A}}$.

Proof. Let ν be a probability measure and ϕ be a function in $L^2(\mathbb{T}^d)$. Then, we can easily verify that

$$\begin{aligned}\Phi^{\mathcal{A}\mathcal{B}}(\nu)(\phi) &= \frac{(\nu)(\mathcal{A}\mathcal{B}\phi)}{(\nu)(\mathcal{A}\mathcal{B}1)} = \frac{(\nu)(\mathcal{A}\mathcal{B}\phi)}{(\nu)(\mathcal{A}1)}\frac{(\nu)(\mathcal{A}1)}{(\nu)(\mathcal{A}\mathcal{B}1)}, \\ &= \frac{\Phi^{\mathcal{A}}(\nu)(\mathcal{B}\phi)}{\Phi^{\mathcal{A}}(\nu)(\mathcal{B}1)} = \Phi^{\mathcal{B}}\Phi^{\mathcal{A}}(\nu)(\phi). \end{aligned} \tag{57}$$

□

Recall the operator $\Phi_n^{\mathcal{K}^{\Delta t}}$ defined in (19), which is a compostion of the Feynman-Kac semigroup $\Phi^{\mathcal{K}^{\Delta t,i}}$ associated with the operator $\mathcal{K}^{\Delta t,i}$; see (18). In the sequel, we prove the operator $\Phi_n^{\mathcal{K}^{\Delta t}}$ satisfies the uniform minorization and boundedness condition with respect to Δt, which guarantees the existence of an invariant measure.

Theorem 3.7. There exists a probability measure η so that the operator $\mathcal{K}^{\Delta t}$ satisfies a uniform minorization and boundedness condition as follows

$$\epsilon\eta(\phi) \le \mathcal{K}^{\Delta t}(\phi)(x) \le \gamma\eta(\phi), \quad \forall x \in \mathbb{T}^d, \forall \phi \in L^2(\mathbb{T}^d), \tag{58}$$

where $0 < \epsilon < \gamma$ is independent with Δt. Moreover, the limit operator when $\Delta t \to 0$, which is just the exact solution operator $\mathcal{U}(T, 0)$, also satisfies this condition.

Proof. We first define an operator $P^{\Delta t} = \prod_{i=0}^{M-1} P_{t_i}^{\Delta t}$, which corresponds to the case when $c(t, \mathbf{x}) = 0$ in Eq.(27). Since $c(t, \mathbf{x})$ is bounded (i.e. $c_1 \le c(t, \mathbf{x}) \le c_2$), one can easily obtain the following estimate based on the Feynman-Kac formula

$$P^{\Delta t}(\phi)e^{c_1 T} \le \mathcal{K}^{\Delta t}(\phi) \le P^{\Delta t}(\phi)e^{c_2 T}. \tag{59}$$

Thus, to estimate the bounds for $\mathcal{K}^{\Delta t}$, we only need to study the operator $P^{\Delta t}$. Moreover, it is sufficient to prove the result for any indicator function of a Borel set $S \subset \mathbb{T}^d$.

We aim to prove that

$$\mathbb{P}(\boldsymbol{X}_M \in S | \boldsymbol{X}_0 = x) \ge \epsilon\eta(S), \tag{60}$$

for a probability measure η and a constant $\epsilon \geq 0$. Here $\boldsymbol{X}_i$ are defined in Eq.(13) as the numerical solution to the SDE (6). The idea of the proof is to explicitly rewrite $\boldsymbol{X}_M$ as a perturbation of the reference evolution corresponding to $\boldsymbol{b} = 0$. According to the SDE scheme (13), we have

$$\boldsymbol{X}_M = \boldsymbol{X}_0 + \boldsymbol{G}_M + \boldsymbol{F}_M, \tag{61}$$

where

$$\boldsymbol{G}_M = \sqrt{2\kappa\Delta t}\sum_{i=0}^{M-1}\boldsymbol{\omega}_i, \quad \text{and,} \quad \boldsymbol{F}_M = \Delta t\sum_{i=0}^{M-1}\boldsymbol{b}(i\Delta t, \boldsymbol{X}_i). \tag{62}$$

We know that $|\boldsymbol{F}_m| \leq T||\boldsymbol{b}||_{L^\infty}$ and $\boldsymbol{G}_M$ is a Gaussian random variable with covariance matrix $2\kappa T\mathrm{Id}_d$. Therefore

$$\begin{aligned}\mathbb{P}(\boldsymbol{X}_M \in S|\boldsymbol{X}_0 = \boldsymbol{x}) &\geq \mathbb{P}(\boldsymbol{G}_M \in S - \boldsymbol{x} - \boldsymbol{F}_M)\\ &= (\frac{1}{2\pi\kappa T})^{d/2}\int_{S-\boldsymbol{x}-\boldsymbol{F}_m}\exp(-\frac{|\boldsymbol{y}|^2}{2\kappa T})d\boldsymbol{y}.\end{aligned} \tag{63}$$

Since the state space $\mathbb{T}^d$ is compact, we can find $R > 0$ such that $|\boldsymbol{x} + F_M| \leq R$ for all $\boldsymbol{x} \in \mathbb{T}^d$. Thus, we define the probability measure η as

$$\eta(S) = Z_R^{-1}\inf_{|Q|\leq R}\int_{S+Q}\exp(-\frac{|\boldsymbol{y}|^2}{2\kappa T})d\boldsymbol{y}, \quad \forall S \subset \mathbb{T}^d, \tag{64}$$

where Z_R is a normalization constant. Setting $\epsilon = Z_R(4\pi\kappa T)^{-d/2}$, we can easily verify that $\eta(S) \geq Z_R^{-1}\exp(-\frac{|R+1|^2}{2\kappa T})|S|$, which satisfies a uniform minorization condition.

The uniform boundedness condition is automatically satisfied since η has a positive density with respect to Lebesgue measure.

The situation when the exact solution operator is considered can be samely proved by changing Eq.(61) into an Ito integration form, namely

$$\mathbf{X}^{T,\mathbf{x}} = \mathbf{X}^{0,\mathbf{x}} + \int_0^T \mathbf{b}(\mathbf{X}^{t,\mathbf{x}}, t)dt + \int_0^T \sqrt{2\kappa}d\mathbf{w}(t)$$

and then go through the same procedure. □

We can now represent an important result that ensures the existence of the limiting messure for the discretized Feymann-Kac dynamics. The detailed proof of Proposition 3.8 can be found in [23], or Corollary 2.5 in [25].

Proposition 3.8. Suppose the minorization and boundedness conditions (58) hold true. Then, the $\Phi_n^{\mathcal{K}^{\Delta t}}$ admits an invariant measure $\nu_{\Delta t}$, whose density function is the eigenfunction of the operator $(\mathcal{K}^{\Delta t})^\star$, adjoint operator of the solution operator $\mathcal{K}^{\Delta t}$. Moreover, for any initial distribution $\nu_0 \in \mathcal{P}(\mathbb{T}^d)$

$$\left|\left|\Phi_n^{\mathcal{K}^{\Delta t}}(\nu_0) - \nu_{\Delta t}\right|\right|_{TV} \leq 2(1 - \frac{\epsilon}{\gamma})^n, \tag{65}$$

where $||\cdot||_{TV}$ is the total variation norm and $0 < \epsilon < \gamma$ are from the minorization and boundedness conditions introduced in (58). In addition this is also true when changing $\mathcal{K}^{\Delta t}$ to the exact solution operator $\mathcal{U}(T, 0)$.

Corollary 3.9. The principal eigenvalue of $K^{\Delta t}$, $\mu_{\Delta t}$ satisfies the following relation

$$e^{\mu_{\Delta t}(\lambda)T} = \nu_{\Delta t}\mathcal{K}^{\Delta t}1 = \Phi_n^{\mathcal{K}^{\Delta t}}(\nu_0)\mathcal{K}^{\Delta t}1 + \rho_n, \tag{66}$$

where ν_0 is any bounded non-negative initial probability measure, T is the period of the time parameter, and $\rho_n = O(1-\frac{\epsilon}{\gamma})^n$.

Proof. Lemma 3.8 implies that for any bounded non-negative measure ν_0, the measure $\Phi_n^{\mathcal{K}^{\Delta t}}(\nu_0)$ converges to an invariant measure $\nu_{\Delta t}$ in the weak sense, that is

$$\nu_{\Delta t}\phi := \int_{\mathbb{T}^d} \phi d\nu_{\Delta t} = \Phi_n^{\mathcal{K}^{\Delta t}}(\nu_0)(\phi) + O(1-\frac{\epsilon}{\gamma})^n, \tag{67}$$

for any bounded non-negative measurable function ϕ.

Then, we take $\phi = \mathcal{K}^{\Delta t}1$. From the fact that the density function of $\nu_{\Delta t}$ is the eigenfunction of the operator $(\mathcal{K}^{\Delta t})^\star$, we get that

$$\nu_{\Delta t}(\mathcal{K}^{\Delta t}1) = ((\mathcal{K}^{\Delta t})^\star \nu_{\Delta t})1 = e^{\mu_{\Delta t}(\lambda)T}(\nu_{\Delta t}1) = e^{\mu_{\Delta t}(\lambda)T}. \tag{68}$$

Thus we finish the proof. □

Now we compute the principal eigenvalue $\mu_{\Delta t}(\lambda)$.

Lemma 3.10. Denote $\nu_{\Delta t}^k = \prod_{i=0}^{k-1} \Phi^{\mathcal{K}^{\Delta t,i}}\nu_{\Delta t}$. Let $e_k = (\nu_{\Delta t}^k)(\mathcal{K}^{\Delta t,k}1)$ denote the changing of mass. Then, we have

$$e^{\mu_{\Delta t}(\lambda)T} = \prod_{k=0}^{M-1} e_k, \quad \text{and} \quad \mu_{\Delta t}(\lambda) = \frac{1}{M\Delta t}\sum_{k=0}^{M-1}\log(e_k). \tag{69}$$

Proof. It is easy to verify that

$$\nu_{\Delta t}^M = \nu_{\Delta t}^0 = \nu_{\Delta t}, \quad (\mathcal{K}^{\Delta t,k})^*\nu_{\Delta t}^k = e_k\nu_{\Delta t}^{k+1}, \tag{70}$$

for some positive numbers e_k's. These e_k's are refer to the changing of the mass for each small step $\mathcal{K}^{\Delta t,k}$. Thus we have $(\mathcal{K}^{\Delta t})^*\nu_{\Delta t}^0 = (\prod_{k=0}^{M-1} e_k)\nu_{\Delta t}^0$, which means $e^{\mu_{\Delta t}(\lambda)T} = \prod_{k=0}^{M-1} e_k$. □

At this moment we are ready to present the main theorem in our paper as follows.

Theorem 3.11. Let $\xi_k^{p,n-1}$, $k = 1, \cdots, M$, $p = 1, \cdots, N$, $n \in \mathbb{Z}^+$, T, Δt be defined in N-IPS system Algrithm 1. Then we have the following convergence:

$$\lim_{N\to\infty}(M\Delta t)^{-1}\sum_{i=1}^{M}\log\left(N^{-1}\sum_{p=1}^{N}\exp(c(t_i,\widetilde{\xi}_i^{p,n-1})\Delta t)\right) = \mu(\lambda) + O((1-\frac{\epsilon}{\gamma})^n) + O((\Delta t)^{\frac{1}{2}}), \tag{71}$$

where ϵ and γ are defined in Proposition 3.8.

Proof. By the theory of N-IPS system, $\{\xi_k^{p,n-1}\}_{p=1,\cdots,N}$ will approximately distributed as $\prod_{i=0}^{k-1}\Phi^{\mathcal{K}^{\Delta t,i}}\Phi_{n-1}^{\mathcal{K}^{\Delta t}}\nu_0$ when $N\to\infty$. Thus the increasing of the mass for each small step $\mathcal{K}^{\Delta t,k}$

$$e_{k,n}^N = N^{-1}\sum_{p=1}^{N}\exp(c(t_k,\widetilde{\xi}_k^{p,n-1})\Delta t), \tag{72}$$

will satisfies

$$\lim_{N\to\infty} e_{k,n}^N = (\prod_{i=0}^{k-1}\Phi^{\mathcal{K}^{\Delta t,i}}\Phi_{n-1}^{\mathcal{K}^{\Delta t}}\nu_0)(\mathcal{K}^{\Delta t,k}1). \tag{73}$$

As Proposition 3.8 stated, $\Phi_{n-1}^{\mathcal{K}^{\Delta t}}\nu_0 = \nu_{\Delta t}+\delta_n$, where $||\delta_n||_{TV}\le 2(1-\frac{\epsilon}{\gamma})^n$, thus

$$\lim_{N\to\infty} e_{k,n}^N = (\prod_{i=0}^{k-1}\Phi^{\mathcal{K}^{\Delta t,i}}\nu_{\Delta t})(\mathcal{K}^{\Delta t,k}1) + O((1-\frac{\epsilon}{\gamma})^n). \tag{74}$$

Combining Lemma 3.10, we conclude that

$$\lim_{N\to\infty}(M\Delta t)^{-1}\sum_{i=1}^{M}\log(e_{k,n}^N) = (M\Delta t)^{-1}\sum_{k=0}^{M-1}\log(e_k) + O((1-\frac{\epsilon}{\gamma})^n) = \mu_{\Delta t}(\lambda) + O((1-\frac{\epsilon}{\gamma})^n). \tag{75}$$

From Theorem 3.5, we know that $|\mu(\lambda)-\mu_{\Delta t}(\lambda)| = O((\Delta t)^{\frac{1}{2}})$, which concludes the proof. □

4. Numerical results

In this section, we first present numerical examples to verify the convergence analysis of the proposed method in computing eigenvalues. Then, we compute the KPP front speeds in 2D and 3D chaotic flows. In addition, we investigate the dependence of the KPP front speed on the magnitude of velocity field and the evolution of the empirical distribution of the N-IPS.

4.1. Convergence tests in computing principal eigenvalue

We first verify the convergence of the operator splitting method in approximating solution operator. Let $\mathbf{x} = (x_1, x_2)^T$. We consider the following two-dimensional non-autonomous equation in $\mathbb{T}^d$:

$$u_t = \mathcal{L}(t)u + \mathcal{C}(t)u, \tag{76}$$

where $\mathbb{T}^d = [0, 2\pi]^2$, $\mathcal{L}(t) = \Delta_{\mathbf{x}} + (\sin(x_2)\cos(2\pi t), \sin(x_1)\cos(2\pi t))\cdot\nabla_{\mathbf{x}}$, and $\mathcal{C}(t) = \big(\sin(x_1+x_2)+\cos(x_1+x_2)\big)\sin(2\pi t)$.

We use spectral method [34] to discretize Eq.(76), in order to obtain an accurate approximation in the physical space of the solution operator of Eq.(76). Let $V_H = \text{span}\{e_{j,k}\}_{j,k\in[-H,H]\cap\mathbb{Z}}$ denote a finite dimensional space spanned by fourier basis functions, where H is a positive integer and $e_{j,k}(q_1,q_2) = e^{2i\pi(jq_1+kq_2)}$. The operators $\mathcal{L}(t)$ and $\mathcal{C}(t)$ are represented in the space

V_H by the matrices $L^H(t)$ and $M^H(t) \in \mathbb{C}^{(2H+1)^2\times(2H+1)^2}$, where their entries are defined by

$$L^H_{(j_1,k_1),(j_2,k_2)}(t) = \int_D e_{j_1,k_1}\mathcal{L}(t)e_{j_2,k_2}dx, \quad M^H_{(j_1,k_1),(j_2,k_2)}(t) = \int_D c(t,x)e_{j_1,k_1}e_{j_2,k_2}dx, \tag{77}$$
$$\forall j_1,k_1,j_2,k_2 \in [-H,H]\cap\mathbb{Z},$$

We use the matrix exponential function $e^{\Delta t L^H(t)}$ to approximate $e^{\Delta t\mathcal{L}(t)}$ and $e^{\Delta t M^H(t)}$ to approximate $e^{\Delta t M(t)}$, respectively. Thus, we get an approximation formula for $\mathcal{K}^{\Delta t}$ as

$$K^{H,\Delta t} = \prod_{j=0}^{T/\Delta t-1} e^{\Delta t L^H(t_j)}e^{\Delta t M^H(t_j)}. \tag{78}$$

For the reference solution, we choose a much finer time step Δt_{ref} and compute the approximation formula

$$\widetilde{K}^{H,\Delta t_{ref}} = \prod_{j=0}^{T/\Delta t_{ref}-1} e^{\Delta t_{ref}(L^H(t_j)+M^H(t_j))}. \tag{79}$$

In this experiment, we choose $H = 24$, $\Delta t = 2^{-1}, 2^{-2}, \cdots, 2^{-9}$, and $\Delta t_{ref} = 2^{-12}$. Then, we compute $||K^{H,\Delta t} - \widetilde{K}^{H,\Delta t_{ref}}||_{L^2}$ to verify our result. Figure 1 shows the convergence results for the splitting method. The convergence rate is $(\Delta t)^{1.05}$. This numerical result suggests that the convergence analysis in Theorem 3.5 is not sharp. More studies on the convergence analysis of our method will be reported in our future work.

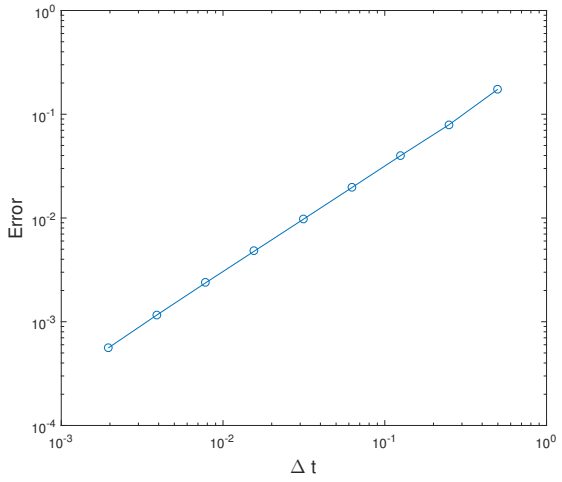

Figure 1: Numerical errors for $||K^{H,\Delta t} - \widetilde{K}^{H,\Delta t_{ref}}||_{L^2}$.

Then, we test the convergence of the Lagrangian method, i.e., Algorithm 1, in computing principal eigenvalues of parabolic-type equations. We still consider the problem (76) with the same $\mathcal{L}(t)$ and $\mathcal{C}(t)$. In this experiment, we choose $\Delta t = 2^{-1}, 2^{-2}, 2^{-3}, 2^{-4}, 2^{-5}$, $N = 200,000$ in the N-IPS system, and iteration number $n = 200$ and $n = 400$ in the Feynman-Kac semigroup iteration method. Figure 9 shows the convergence of principal eigenvalues with

respect to Δt by spectral method and our Lagrangian method, where the reference solution is calculated from spectral method with a finer grid $\Delta t_{ref} = 2^{-8}$. So given sufficient large N and n, the error in calculating principal eigenvalues of linearized KPP operator $\mathcal{A}$ via our proposed Lagrangian approach only comes from the error of operator splitting. Also as the Lagrangian method will eventually converges to some invariant measure approximating the ground truth invariant measure, there is no error accumulation for long time integration.

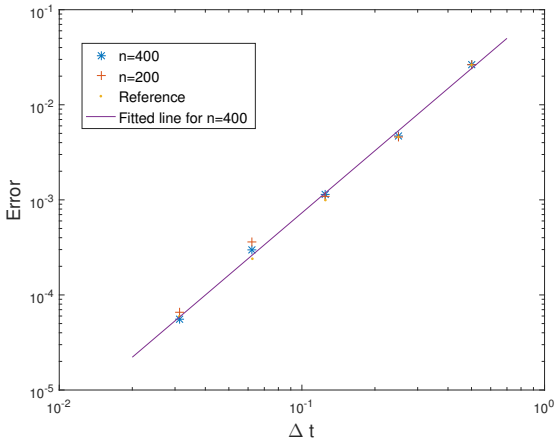

Figure 2: In the Lagrangian method, iteration number $n = 200$ and $n = 400$. The reference solution is obtained by the spectrum method.

4.2. Computing KPP front speeds in different flows

We first compute the KPP front speeds in two different time-independent flows, i.e., a 2D steady cellular flow and a 3D ABC flow. Let $\mathbf{x} = (x_1, ..., x_d)^T$ with $d = 2, 3$. We use the Lagrangian method to compute the following principal eigenvalue problem with periodic boundary condition

$$\kappa \Delta_{\mathbf{x}} \Phi + (2\kappa\lambda \mathbf{e} + \mathbf{v}) \cdot \nabla_{\mathbf{x}} \Phi + \big(\kappa\lambda^2 + \lambda \mathbf{e} \cdot \mathbf{v} + \tau^{-1} f'(0)\big)\Phi = \mu(\lambda)\Phi, \quad \mathbf{x} \in [0, 2\pi)^d \tag{80}$$

$f(u) = u(1-u)$, and $(\mu(\lambda), \Phi)$ are principal eigenvalue of (80) and its associated eigenfunction, respectively. The velocity field $\mathbf{v} = (-\sin x_1 \cos x_2, \cos x_1 \sin x_2)$ in the 2D steady cellular flow, and $\mathbf{v} = (\sin x_3 + \cos x_2, \sin x_1 + \cos x_3, \sin x_2 + \cos x_1)$ in the 3D ABC flow.

We choose the parameters $\kappa = 1$ and $\tau = 1$ in (80). We use the spectral method to obtain an accurate reference solution for the principal eigenvalue of (80). Figure 3 shows the convergence results of the Lagrangian method in computing the principal eigenvalue, where $\lambda = 0.35$ for the 2D cellular flow and $\lambda = 0.55$ for the 3D ABC flow. We find the convergence rate of the Lagrangian method is $(\Delta t)^{1.51}$ for the 2D steady cellular flow, and $(\Delta t)^{1.70}$ for the 3D ABC flow. Thus, we can use the Lagrangian method to compute the KPP front speeds in both 2D and 3D flows.

After getting the principal eigenvalue, we compute the KPP front speed c^* through the formula $c^* = \inf_{\lambda>0} \frac{\mu(\lambda)}{\lambda}$. We only show the numerical results for the 3D ABC flow here since

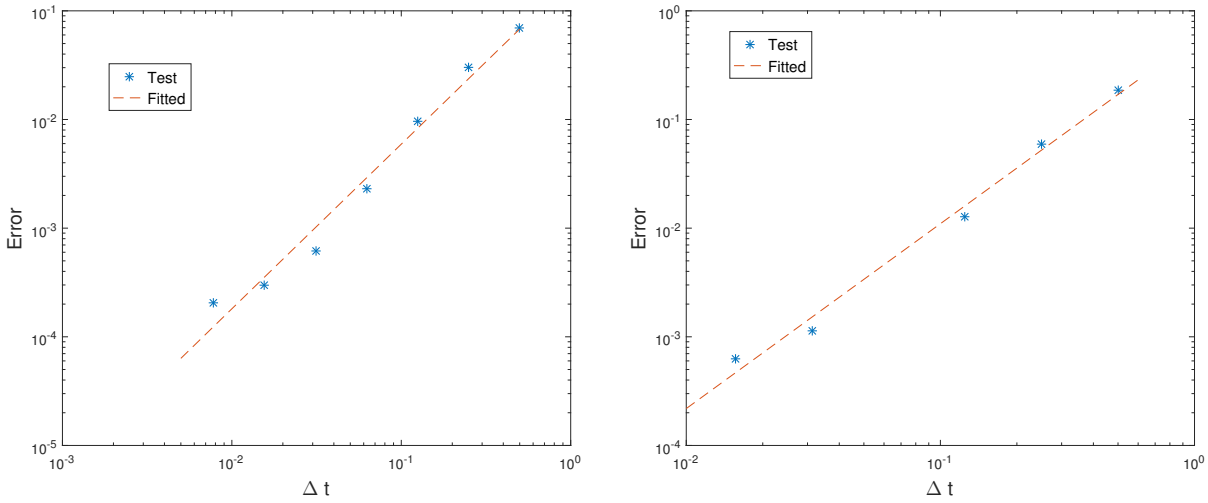

(a) 2D convergence test, fitted slope ≈ 1.51

(b) 3D convergence test, fitted slope ≈ 1.60.

Figure 3: Errors of the principal eigenvalue computed by using different time steps.

the results for the 2D steady cellular flow is quantitatively similar. We choose the velocity field $\mathbf{v} = A(\sin x_3 + \cos x_2, \sin x_1 + \cos x_3, \sin x_2 + \cos x_1)$, where A is the strength of the convection. In Figure 4, we show the results of $\frac{\mu(\lambda)}{\lambda}$ for ABC flows with $A = 1$ and $A = 10$. The amplitude of the principal eigenvalue increases fast and the convergence speed becomes slower. Notice that in this case, the flow becomes much more unstable since the convection becomes dominant comparing to the diffusion. We will study this issue in subsection 4.3.

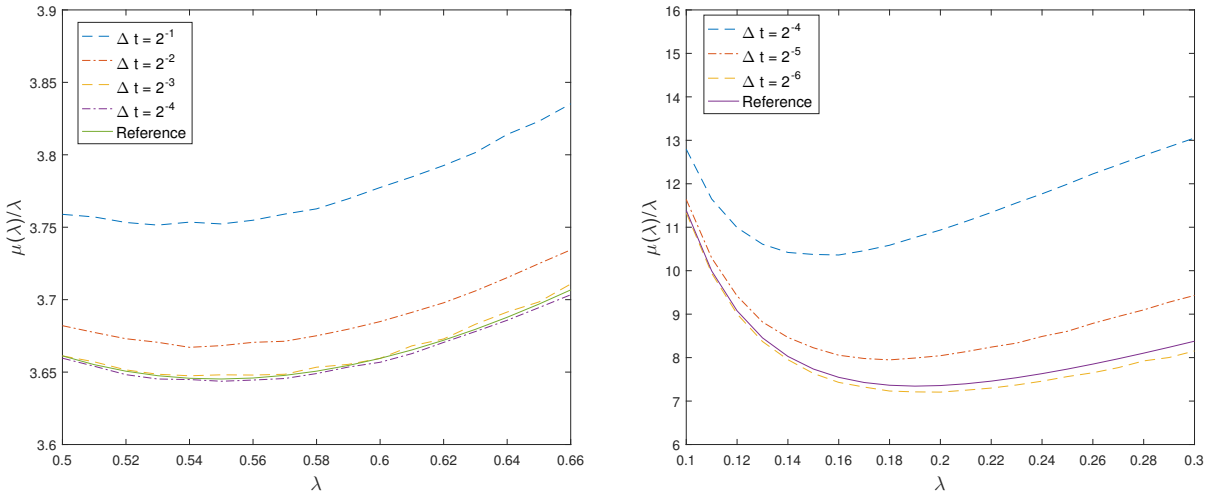

(a) A = 1

(b) A = 10

Figure 4: Numerical results of $\frac{\mu(\lambda)}{\lambda}$ for different λ's in the ABC flow.

Next, we compute the KPP front speed in a 2D unsteady (time-dependent) cellular flow. Let $\mathbf{x} = (x_1, x_2)^T$. We use the Lagrangian method to compute the following principal eigen-

value problem with periodic boundary condition

$$\kappa\Delta_{\mathbf{x}}\Phi + (2\kappa\lambda\mathbf{e} + \mathbf{v})\cdot\nabla_{\mathbf{x}}\Phi + \big(\kappa\lambda^2 + \lambda\mathbf{e}\cdot\mathbf{v} + \tau^{-1}f'(0)\big)\Phi - \Phi_t = \mu(\lambda)\Phi, \quad (t,\mathbf{x}) \in [0,T]\times[0,2\pi)^2 \tag{81}$$

T is the period of $\mathbf{v}$ in t, $f(u) = u(1-u)$, and $(\mu(\lambda), \Phi)$ are principal eigenvalue of (81) and its associated eigenfunction, respectively. The velocity field of the 2D unsteady cellular flow $\mathbf{v} = \big(-\sin x_1 \cos x_2(1+\delta\cos 2\pi t), \cos x_1 \sin x_2(1+\delta\cos 2\pi t)\big)$, where $\delta > 0$ is a parameter.

We choose the parameters $\kappa = 1$ and $\tau = 1$ in (81) and $\delta = 0.5$ in the velocity field $\mathbf{v}$. We use the spectral method to obtain an accurate reference solution for the principal eigenvalue of (81). For figure 5a, we choose $\lambda = 0.57$. Figure 5a shows the convergence results of the Lagrangian method in computing the principal eigenvalue, where the convergence rate is $(\Delta t)^{1.31}$. Figure 5b shows the numerical results of $\frac{\mu(\lambda)}{\lambda}$ for different λ's, from which we can compute the KPP front speed in the 2D unsteady cellular flow. We could see that $\frac{\mu(\lambda)}{\lambda}$ is convex within the calculate interval, hence we can compute the KPP front speed by minimizing $\frac{\mu(\lambda)}{\lambda}$ on the computed mesh of λ.

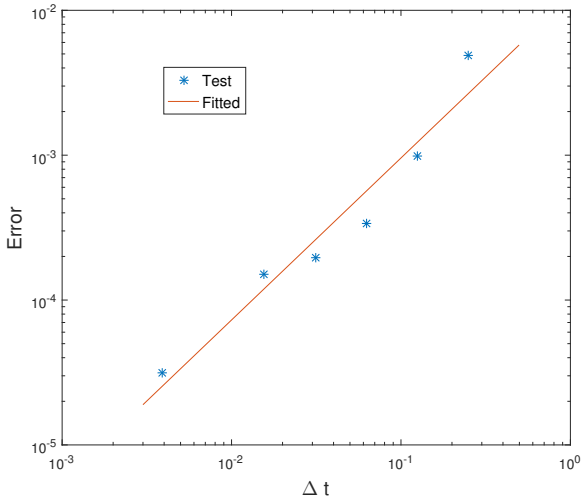

(a) Convergence test for different Δt's. The fitted slope is ≈ 1.31.

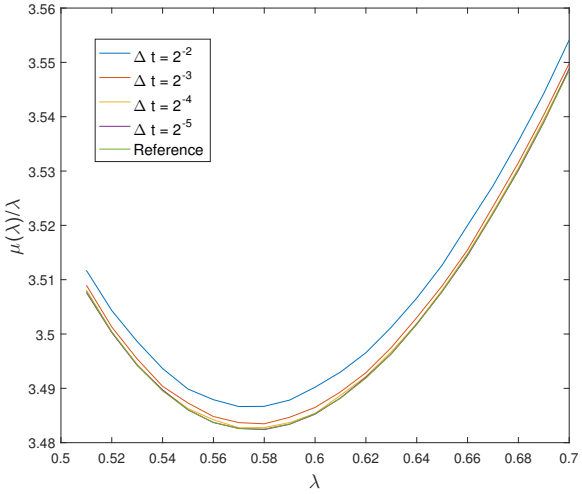

(b) Numerical results of $\frac{\mu(\lambda)}{\lambda}$ for different λ's.

Figure 5: Numerical results for a 2D unsteady cellular flow.

4.3. Investigate the dependence of front speed on the strength of the flows

To further test the performance of the Lagrangian method, we study the dependence of the KPP front speeds on the strength of different flows. Let us first consider this issue in KPP front speeds of time-independent flows. If we scale $\mathbf{v} \to A\mathbf{v}$, Eq.(80) can be rewritten as the following form

$$\kappa\Delta_{\mathbf{x}}\Phi + (2\kappa\lambda\mathbf{e} + A\mathbf{v})\cdot\nabla_{\mathbf{x}}\Phi + \big(\kappa\lambda^2 + \lambda\mathbf{e}\cdot A\mathbf{v} + \tau^{-1}f'(0)\big)\Phi = \mu(\lambda)\Phi, \quad \mathbf{x}\in\mathbb{T}^d \tag{82}$$

The KPP front speed is $c^* = \inf_{\lambda>0}\frac{H(\lambda)}{\lambda}$. Notice that the KPP front speed c^* depends on A, i.e., $c^* = c^*(A)$. We will study this issue by the Lagrangian method.

We consider the equivalent equation

$$\kappa A^{-1}\Delta_{\mathbf{x}}\Phi + (2\kappa A^{-1}\lambda\mathbf{e} + \mathbf{v})\cdot\nabla_{\mathbf{x}}\Phi + \left(\kappa A^{-1}\lambda^2 + \lambda\mathbf{e}\cdot\mathbf{v} + \tau^{-1}f'(0)A^{-1}\right)\Phi = \widetilde{\mu}(\lambda)\Phi, \quad \mathbf{x}\in\mathbb{T}^d \tag{83}$$

where $\widetilde{\mu}(\lambda) = A^{-1}\mu(\lambda)$. Let $\widetilde{c}^*$ denote the KPP front speed of the rescaled equation (83). We have that

$$\widetilde{c}^* = \inf_{\lambda>0}\frac{\widetilde{\mu}(\lambda)}{\lambda} = \frac{c^*}{A}. \tag{84}$$

We choose the parameters $\kappa = 1$ and $\tau = 1$ in (83) and denote $\sigma = A^{-1}$. For the 2D steady cellular flow $\mathbf{v} = (-\sin x_1\cos x_2, \cos x_1\sin x_2)$, it has proven that $c^*(A) = O(A^{1/4})$. So we have that $\widetilde{c}^*(\sigma) = \sigma O(\sigma^{-1/4}) = O(\sigma^{3/4})$, which provides a theoretical guidence for our numerical experiments. For other flows, such as 3D chaotic flows and time-dependent flows, the understanding of $c^*(A)$ for large A's (or $\widetilde{c}^*(\sigma)$ for small σ's) remains open. We will study these flows here.

Figure 6a shows the numerical results of $\widetilde{c}^*(\sigma)$ in the 2D steady cellular flow. With the numerical results, we compute regression and obtain $\widetilde{c}^*(\sigma) = O(\sigma^{0.74})$. We also investigate $\widetilde{c}^*(\sigma)$ for σ in 3D Kolmogorov flow, where $\mathbf{v} = (\sin x_1, \sin x_2, \sin x_3)$. Figure 6b shows the numerial results for the 3D Kolmogorov flow. We obtain that $\widetilde{c}^*(\sigma) = O(\sigma^{0.43})$. It corresponds to the effective diffusivity result of Kolmogorov flow in [39] given that estimate between effective diffusivities and KPP front speed in large A regime is correct in 3D. To the best of our knowledge, such analytical result is only proved in 2D; see [32].

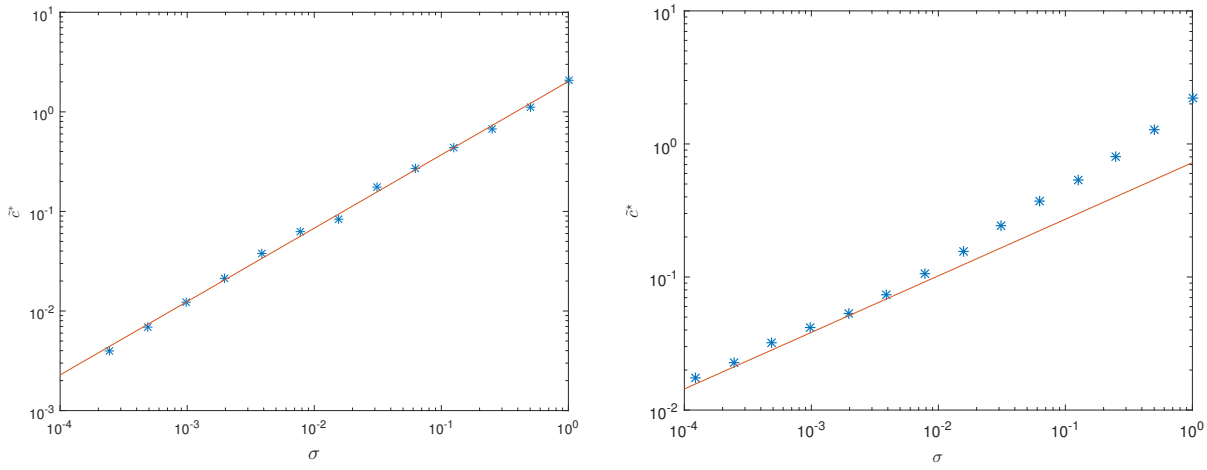

(a) Numerical results of $\widetilde{c}^*(\sigma)$ in 2D cellular flow. The fitted slope is ≈ 0.74.

(b) Numerical results of $\widetilde{c}^*(\sigma)$ in 3D K flow. The fitted slope is ≈ 0.43.

Figure 6: Numerical results of $\widetilde{c}^*(\sigma)$ in different flows.

Next, we study the dependence of the KPP front speeds on the strength of time-dependent flows. In the 2D experiment, we choose $\mathbf{v} = (-\cos x_2 - \theta\sin x_1\cos(2\pi t), \cos x_1 + \theta\sin x_2\cos(2\pi t))$, which is refered to as the 2D time-periodic mixing flow. In the 3D experiments, we will consider two flows. The first one is a time-dependent K flow with $\mathbf{v} = \big(\sin(x_3 + \theta\sin(2\pi t)), \sin(x_1 +$

$\theta\sin(2\pi t)), \sin(x_2+\theta\sin(2\pi t))\big)$, and the second one is a time-dependent ABC flow with $\mathbf{v} = \big(\sin(x_3+\sin(2\pi\Omega t))+\cos(x_2+\sin(2\pi\Omega t)), \sin(x_1+\sin(2\pi\Omega t))+\cos(x_3+\sin(2\pi\Omega t)), \sin(x_2+\sin(2\pi\Omega t))+\cos(x_1+\sin(2\pi\Omega t))\big)$.

For the 2D time-periodic mixing flow, we choose the iteration time $n = 100$, time step $\Delta t = 2^{-9}$ and particle number $N = 400,000$. Figure 7a shows the result of $\widetilde{c}^*(\sigma)$ for small σ's and different θ's.

For the 3D time-dependent K flow, we choose iteration time $n = 256$, time step $\Delta = 2^{-7}$ and particle number $N = 400,000$. Figure 7b shows the result of $\widetilde{c}^*(\sigma)$ for small σ's and different θ's. Again given estimate discussed in time-independent part is correct, it corresponds to effective diffusivity result in [38]. For the 3D time-dependent ABC flow, we use $N = 250,000$ particles to simulate for time up to $n = 2^{15}, dt = 2^{-6}$. $\Omega = 2^{-7}$ to 2^0. Figure 8 shows our result.

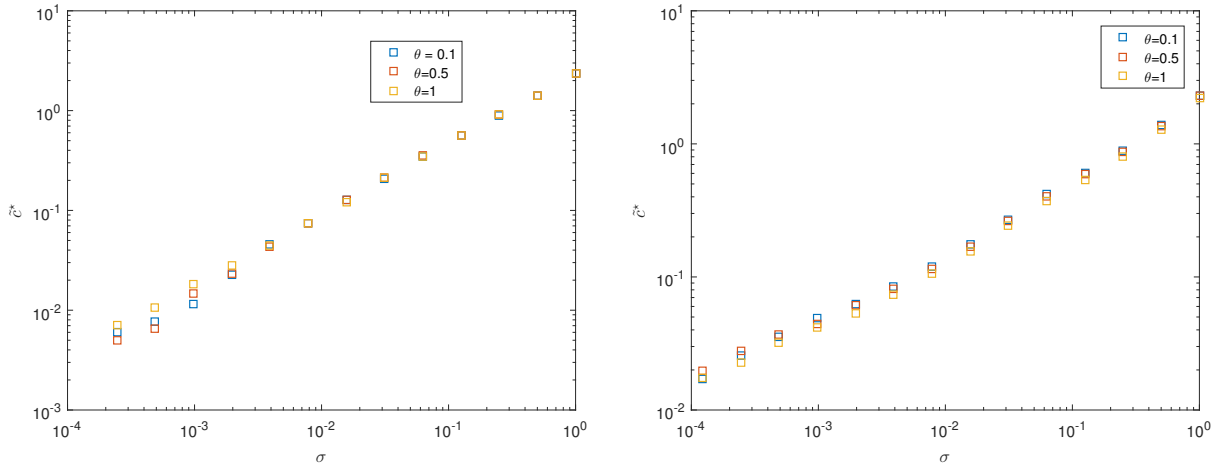

(a) Numerical results of $\widetilde{c}^*(\sigma)$ in a 2D Cat-eye flow.

(b) Numerical results of $\widetilde{c}^*(\sigma)$ in a 3D time-dependent K flow.

Figure 7: Numerical results of $\widetilde{c}^*(\sigma)$ in different flows.

In Figure 10, we plot out procedure searching for the λ when the minimal in Eq.(84) was reached. We use $a\lambda + b\lambda^{-1} + c$ to fit a curve, then find the minimum of the curve. When σ is large, the relative flutuation is small and the minimun is easily to be find. When σ is small, the relative flutuation becomes strong enough, so we decide to fit the curve, then find the minimun point.

4.4. Evolution of the empirical distribution of the particles

As stated in Theorem 3.8, the empirical distribution converges to the invariant measure of Feynman-Kac semigroup as n approaches infinity. Our Lagrangian method can not only calculate the principal eigenvalue but also compute the evolution of the distribution. In this subsection, we will study the empirical distribution of the N-IPS system moduled to torus space.

Figure 11 shows the invariant distribution generated by the N-IPS system in the 2D steady cellular flow. The parameter σ varies from 2^0 to 2^{-5}. The strength of the convection

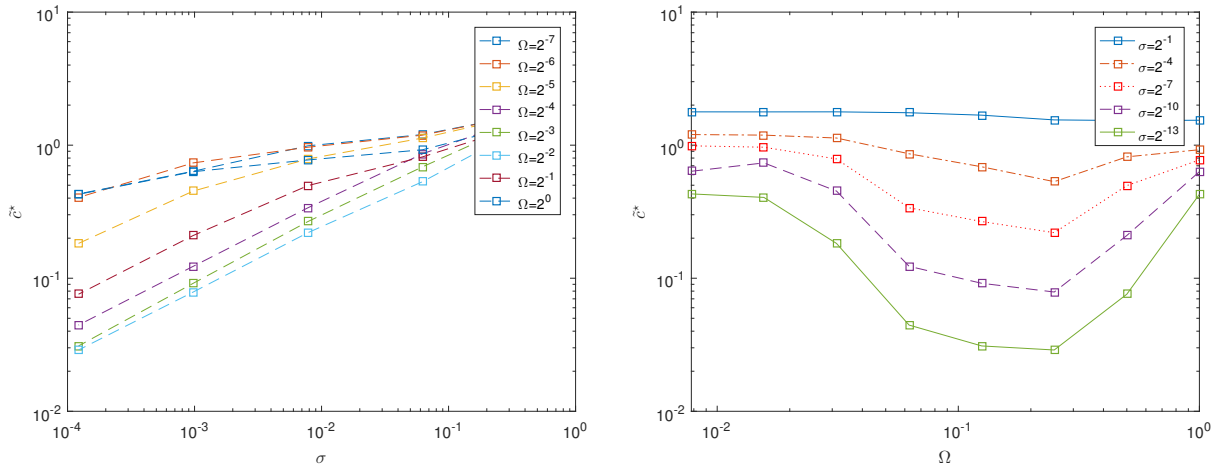

(a) Numerical results of $c^*(\sigma)$ for different Ω and different σ (b) Numerical results of $\widetilde{c}^*(\sigma)$ for different Ω and different σ.

Figure 8: Numerical results of $\widetilde{c}^*(\sigma)$ for different Ω's and different σ's.

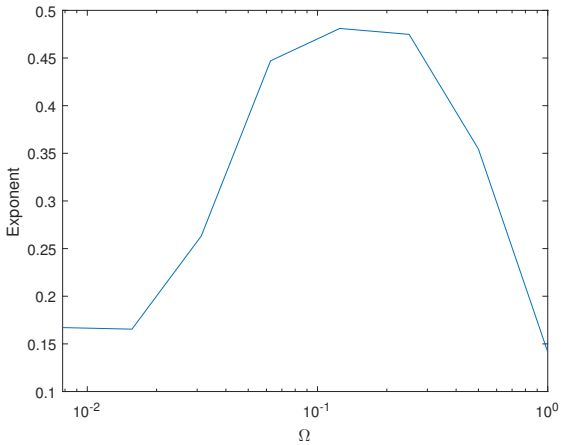

Figure 9: Lyapunov exponent of different Ω in the determinant flow ($\sigma = 0$).

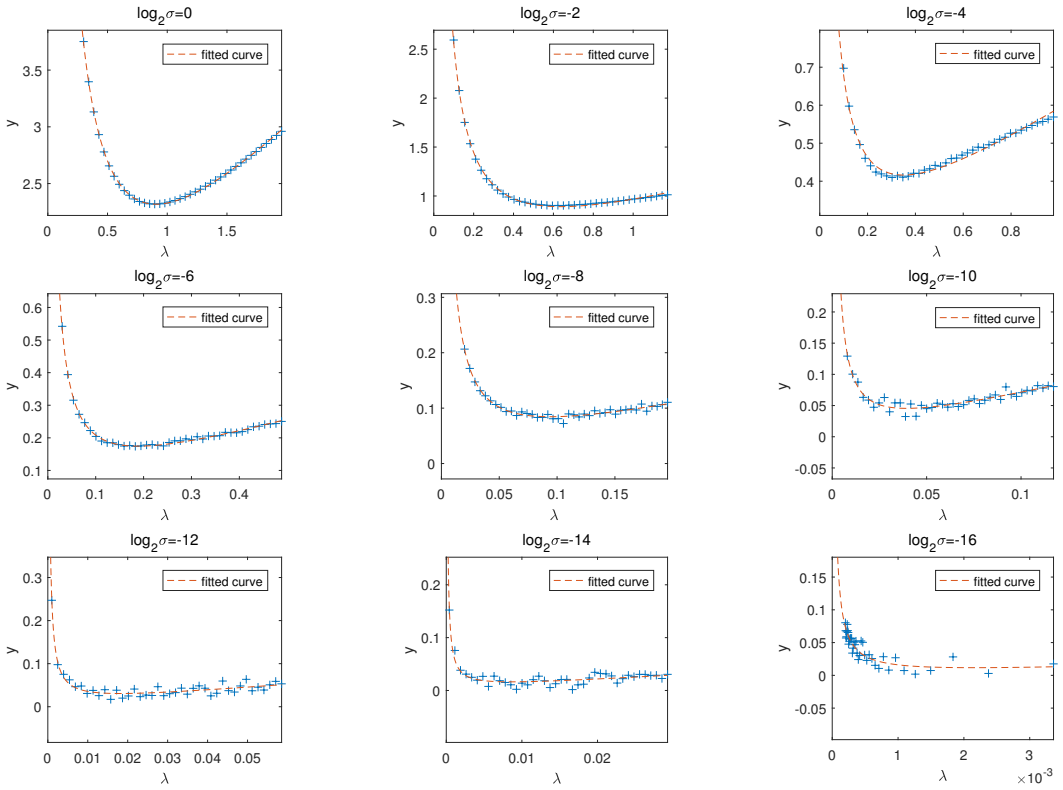

Figure 10: Numerical results of $\frac{\mu(\lambda)}{\lambda}$ for different λ's and σ's in the 3D time-dependent K flow. The red dash curve is fitted by $a\lambda + b\lambda^{-1} + c$.

is then proportion to $1/\sigma$. Then we can see from the graph when increasing the strength, the main part of invariant measure gets into a smaller domain and the gradient becomes sharper, which is a common phenomenon in fluid dynamics. In addition, by comparing to the pattern at the boundary of the plot, one can find that the invariant measure is periodic in physical space.

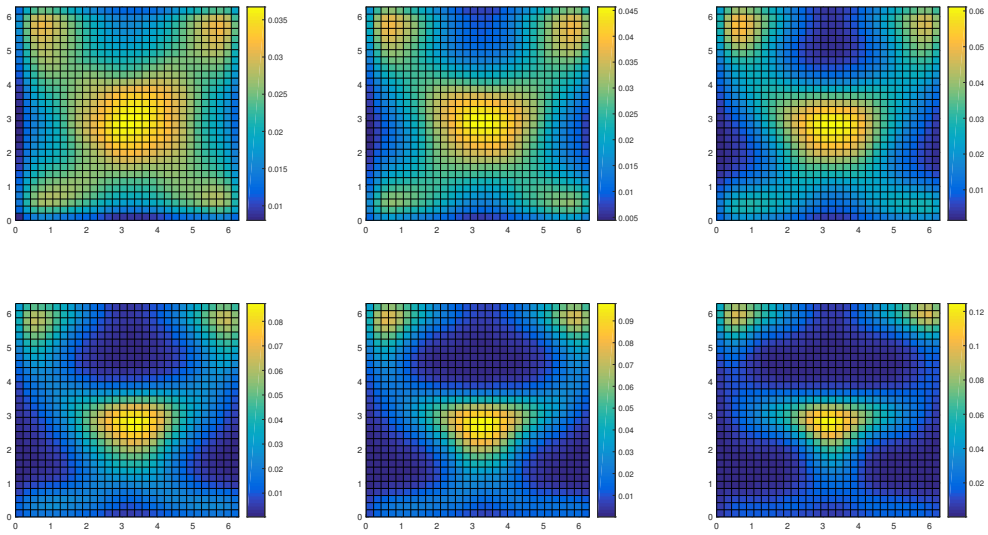

Figure 11: Empirical distributions for the 2D steady cellular flow with σ varies from 2^0 to 2^{-5}. First row from left to right: $\sigma = 2^0$, $\sigma = 2^{-1}$, and $\sigma = 2^{-2}$. Second row from left to right: $\sigma = 2^{-3}$, $\sigma = 2^{-4}$, and $\sigma = 2^{-5}$.

Figure 12 shows the changes of invariant distribution generated by our N-IPS system in a 2D periodic case, it is captured in different time within the period at $n = 400$. From these numerical results, we can see the invariant distribution varies at different times of one period. But as the starting time of different periods, the first and last subfigure are identical. These are consistent with our expectation obtained in Lemma 3.10, where we proved that the invariant measure changes periodically with the same period as the flow.

Figure 13 shows the invariant distribution generated by the N-IPS system in the 2D unsteady periodic flow. The parameter σ varies from 2^0 to 2^{-5}. This is similar to the results shown in Figure 11, showing that with the increasing of the strength of the convection, the invariant measure becomes compact supported with a sharp gradient.

The observation from the plots of invariant measure is twofold. First, the invariant measure of the KPP operator is no longer uniform distribution. This is due to the resampling effect from $c(x, t)$. Second, the invariant measure quantitatively turns to some limiting measure as $\sigma \to 0$. And when σ is small, the invariant measure develops sharp gradients, which indicates that we may need more particles to calculate the eigenvalue accurately. Moreover, it may take more iteration time steps to converges. Effectively sampling the invariant measure for the KPP operator will be studied in our future works.

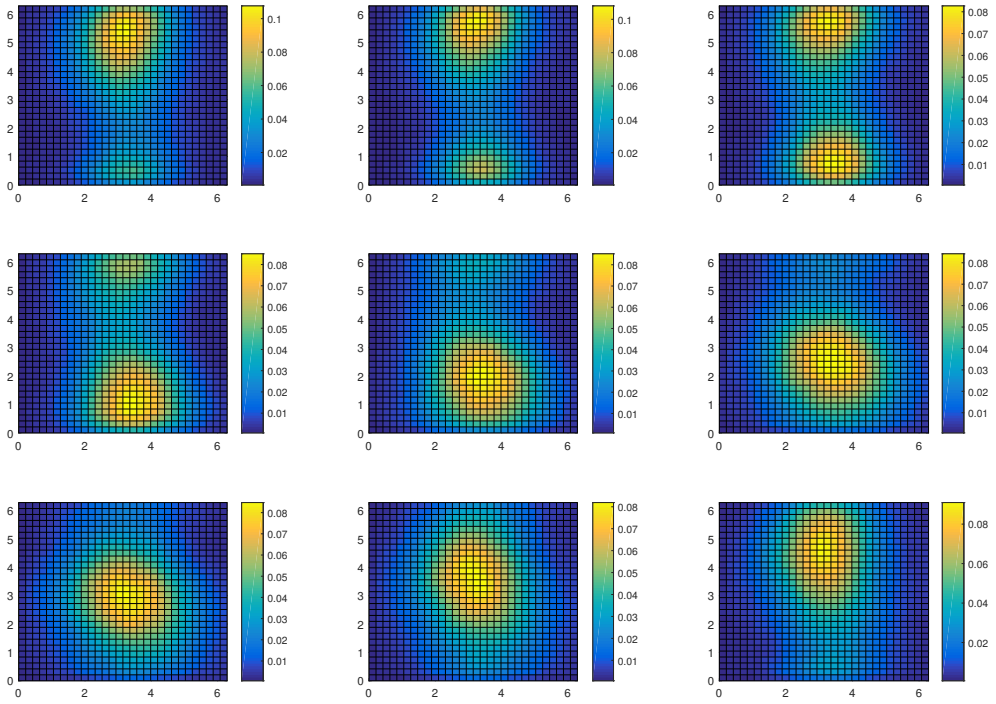

Figure 12: Empirical distributions for the 2D time-periodic mixing flow with $\theta = 1$, $\sigma = 1$, in different phase of one period: t varies from 0 to 1 with time interval equal to $1/9$.

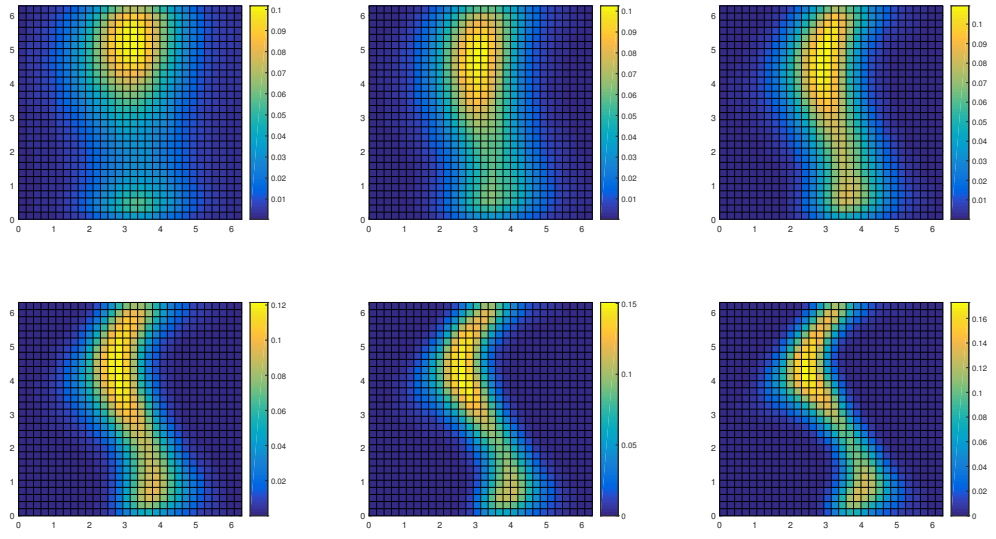

Figure 13: Empirical distributions for the 2D time-periodic mixing flow with $\theta = 1$, σ varies from 2^0 to 2^{-5}. First row from left to right: $\sigma = 2^0$, $\sigma = 2^{-1}$, and $\sigma = 2^{-2}$. Second row from left to right: $\sigma = 2^{-3}$, $\sigma = 2^{-4}$, and $\sigma = 2^{-5}$.

5. Conclusion

In this paper, we developed efficient Lagrangian methods to compute the KPP front speeds in time-periodic cellular and chaotic flows. In addition, we provided rigorous convergence analysis for the numerical schemes. In the convergence analysis, we first analyzed the error of the operator splitting methods in approximating the solution operator corresponding to the linearized KPP equation. Then, we provided the convergence of the Lagrangian method in computing the principal eigenvalue based on the Feynman-Kac semigroup theory. Finally, we presented numerical results to verify the convergence rate of the proposed method for computing the principal eigenvalues. In addition, we computed the KPP front speeds in incompressible time-periodic cellular and chaotic flows both in 2D and 3D spaces.

There are two directions we plan to explore in our future work. First, we shall extend the Lagrangian method to compute the KPP front speeds in complex fluid flows, where the computational domain is not compact. This type of problem is more challenging both analytically and numerically. As stated in the introduction part, there is limited literature on studying the existence of KPP front speeds in complex flows. In the aspect of numerical computation, our current method cannot be adapted to non-compact domains. We shall adopt some relaxation techniques to address this problem. In addition, we shall develop adaptive sampling methods for our Lagrangian methods in order to resolve the sharp gradients in the invariant measure when the magnitude of the velocity field is large.

Acknowledgement

The research of J. Lyu and Z. Wang are partially supported by the Hong Kong PhD Fellowship Scheme. The research of J. Xin is partially supported by NSF grants DMS-1211179, DMS-1522383, DMS-1924548, DMS-1952644, and IIS-1632935. The research of Z. Zhang is supported by Hong Kong RGC grants (Projects 17300817 and 17300318), Seed Funding Programme for Basic Research (HKU), and Basic Research Programme (JCYJ20180307151603959) of The Science, Technology and Innovation Commission of Shenzhen Municipality. The computations were performed using the HKU ITS research computing facilities that are supported in part by the Hong Kong UGC Special Equipment Grant (SEG HKU09).

Appendix A. Error bounds for exponential operator splitting in non-autonomous evolution equations

Appendix A.1. Euler methods for non-autonomous evolution equations

In this section, we review the fundamental rsults for abstract linear evolution equations by semigroup theory; see e.g. [9, 4] for more details. We consider the non-autonomous Cauchy problem (NCP) as follows

$$\begin{cases} \dfrac{d}{dt}u(t) = \mathcal{A}(t)u(t), \quad t \geq s \in \mathbb{R} \\ \quad u(s) = x \in X, \end{cases} \tag{A.1}$$

where X is a Banach space and $(\mathcal{A}(t), \mathcal{D}(\mathcal{A}(t)))_{t\in\mathbb{R}}$ is a family of linear operators on X.

Definition Appendix A.1. A continuous function $u : [s, \infty) \longrightarrow X$ is called a classical solution of (A.1) if $u \in C^1([s, \infty); X), u(t) \in \mathcal{D}(\mathcal{A}(t))$ for all $t \geq s$, $u(s) = x$, and $\frac{d}{dt}u(t) = \mathcal{A}(t)u(t)$ for all $t \geq s$.

Definition Appendix A.2. For a family $(\mathcal{A}(t), \mathcal{D}(\mathcal{A}(t)))_{t\in\mathbb{R}}$ of linear operators on a Banach space X, the NCP (A.1) is well-posed with regularity subspace $(Y_s)_{s\in\mathbb{R}}$ and exponentially bounded solutions, if

(i) (Existence) For all $s \in R$ the subspace

$$Y_s = \{y \in X : \text{there exists a classical solution for the NCP (A.1)}\} \subset \mathcal{D}(\mathcal{A}(s)) \quad \text{(A.2)}$$

is dense in X.

(ii) (Uniqueness) For every $y \in Y_s$, the solution $u_s(\cdot, y)$ is unique.

(iii) (Continuous dependence) The solution continuously depends on s and y, i.e., if $s_n \to s \in \mathbb{R}, ||y_n - y||_X \to 0$ with $y_n \in Y_{y_n}$, then we have $||\hat{u}_{s_n}(t, y_n) - \hat{u}_s(t, y)||_X \to 0$ uniformly for t in compact subsets of $\mathbb{R}$, where

$$\hat{u}_s(t, y) = \begin{cases} u_r(t, y) & if\ r \leq t, \\ y & if\ r > t. \end{cases}$$

(iv) (Exponential boundedness) There exists a constant $\omega \in \mathbb{R}$ such that

$$||u_s(t, y)||_X \leq e^{\omega(t-s)}||y||_X$$

for all $y \in Y_s$ and $t \geq s$.

Definition Appendix A.3. A family $\{\mathcal{U}(t, s), t \geq s\}$ of linear, bounded solution operators on Banach space X is called an exponentially bounded evolution family if

(i) $\mathcal{U}(t, r)\mathcal{U}(r, s) = \mathcal{U}(t, s)$ and $\mathcal{U}(t, t) = Id$ hold for all $t \geq r \geq s \in \mathbb{R}$,

(ii) the mapping $(t, s) \to \mathcal{U}(t, s)$ is strongly continuous,

(iii) $||\mathcal{U}(t, s)||_X \leq e^{\omega(t-s)}$ for some $\omega \in \mathbb{R}$ and all $t \geq s \in \mathbb{R}$.

In contrast to the behavior of C_0-semigroups, the algebraic proposition of an evolution family do not imply any differentiability on a dense subspace. Therefore, we need extra assumptions in order to solve an NCP.

Definition Appendix A.4. An evolution family $\{\mathcal{U}(t, s), t \geq s\}$ is called evolution family solving NCP (A.1) if for every $s \in \mathbb{R}$ the regularity space

$$Y_s = \{y \in X : [s, \infty) \ni t \mapsto \mathcal{U}(t, s)y \text{ solves NCP (A.1)}\}$$

is dense in X.

In this case, the unique classical solution of the NCP (A.1) is given by $u(t) = \mathcal{U}(t, s)x$. The well-posedness of the NCP (A.1) can now be characterized by the existence of solving an evolution family $\{\mathcal{U}(t, s), t \geq s\}$.

Proposition Appendix A.5. Let X be a Banach space and $(\mathcal{A}(t), \mathcal{D}(\mathcal{A}(t)))_{t\in\mathbb{R}}$ be a family of linear operators on X. The following assertions are equivalent [9].

(i) The NCP (A.1) is well-posed.
(ii) There exits a unique evolution family $\{\mathcal{U}(t,s), t \geq s\}$ solving the NCP (A.1).

In addition, if $||e^{\tau\mathcal{A}(t)}||_X \leq e^{\omega\tau}$ for any $\tau \geq 0, t \in \mathbb{R}$, then we have $||\mathcal{U}(t,s)||_X \leq e^{\omega(t-s)}$.

The well-posedness of non-autonomous evolution equations is complicated and there is no general theory describing it. Conditions implying well-posedness are generally divided into parabolic-type assumptions and hyperbolic-type ones. Due to the property of the KPP equation, we only study the parabolic-type conditions in this paper, where the domain $(\mathcal{D}(\mathcal{A}(t))$ is independent of $t \in \mathbb{R}$. We refer the interested reader to [33] for more general cases.

Assumption Appendix A.6. (Parabolic-type conditions)

(P1) The domain $\mathcal{D} = \mathcal{D}(\mathcal{A}(t))$ is independent of $t \in \mathbb{R}$.
(P2) For each $t \in R$ the operator $\mathcal{A}(t)$ is sectorial and generates an analytic semigroup $e^{\cdot\mathcal{A}(t)}$. For all $t \in \mathbb{R}$, the resolvent $\mathcal{R}(\gamma_1, \mathcal{A}(t))$ exists for all $\gamma_1 \in \mathbb{C}$ with Real$\gamma_1 \geq 0$ and there is a constant $M \geq 1$ such that

$$\big|\big|R(\gamma_1, \mathcal{A}(t))\big|\big|_X \leq \frac{M}{|\gamma_1| + 1} \tag{A.3}$$

for Real$\gamma_1 \geq 0$ and $t \in \mathbb{R}$. The semigroups $e^{\cdot\mathcal{A}(t)}$ satisfy $||e^{\tau\mathcal{A}(t)}||_X \leq e^{\omega\tau}$ for some constant $\omega \in \mathbb{R}$.
(P3) There exist constants $L \geq 0$ and $0 < \theta \leq 1$ such that

$$\big|\big|(\mathcal{A}(t) - \mathcal{A}(s))\mathcal{A}(0)^{-1}\big|\big|_X \leq L|t-s|^\theta, \text{ for all } t, s \in \mathbb{R}. \tag{A.4}$$

To obtain a convergence estimate for the operator in certain norm, we need an additional assumption on $\mathcal{A}(t)$ as follows.

Assumption Appendix A.7. The operator $\mathcal{A}(t)$ satisfies a Hölder continuous condition. Namely, there exists $0 \leq \alpha < \beta$ such that for any $x \in \mathcal{D}(\mathcal{A})$,

$$\big|\big|(\mathcal{A}(t) - \mathcal{A}(s))x\big|\big|_X \leq C|t-s|^\beta ||\mathcal{A}(\tau)x||_X^\alpha ||x||_X^{1-\alpha}, \tag{A.5}$$

for any $s \leq \tau \leq t$.

For forward Euler type discretization, Assumption Appendix A.7 can be relaxed to $\tau = s$ only. The backword Euler type discretization needs $\tau = t$, and other discretization methods need different τ's instead. For analytic semigroups, the following estimate holds ture [9, 31].

Lemma Appendix A.8. Let $e^{t\mathcal{A}}$ be an anlytical semigroup on X. Let $\mathcal{A}$ be the infinitesimal generator. There is a constant $C \geq 0$ such that

$$||\mathcal{A}e^{t\mathcal{A}}||_X \leq \frac{C}{t}, \quad t > 0, \quad 0 \leq \alpha \leq 1. \tag{A.6}$$

Now we state the first result, which gives the approximation error of the freezing time coefficients methods for solving the NCP (A.1).

Theorem Appendix A.9. Suppose assumptions Appendix A.6 and Appendix A.7 hold true. Let $\mathcal{U}(T,0)$ be the solution operator associated with the NCP (A.1). Then the solution operator obtained by the freezing time coefficients methods has the following approximation error to $\mathcal{U}(T,0)$

$$\big|\big|\mathcal{U}(T,0)-\prod_{k=0}^{M-1}e^{\Delta t\mathcal{A}(k\Delta t)}\big|\big|_X\leq C(T)(\Delta t)^{\beta-\alpha}, \tag{A.7}$$

where $T>0$, M is an integer, and $\Delta t=\frac{T}{M}$.

Proof. First we refer to [33] for the abstract version of the method of freezing coefficients,

$$\mathcal{U}(t,s)=e^{(t-s)\mathcal{A}(s)}+\int_s^t\mathcal{U}(t,\tau)(\mathcal{A}(\tau)-\mathcal{A}(s))e^{(\tau-s)\mathcal{A}(s)}d\tau \tag{A.8}$$

which immediately gives us that, for every $x\in X$,

$$\begin{aligned}&\big|\big|(\mathcal{U}(t,s)-e^{(t-s)\mathcal{A}(s)})x\big|\big|_X\\ =&\big|\big|\int_s^t\mathcal{U}(t,\tau)(\mathcal{A}(\tau)-\mathcal{A}(s))e^{(\tau-s)\mathcal{A}(s)}xd\tau\big|\big|_X\\ \leq&\int_s^t\big|\big|\mathcal{U}(t,\tau)\big|\big|_X(\tau-s)^\beta\big|\big|\mathcal{A}(s)e^{(\tau-s)\mathcal{A}(s)}x\big|\big|_X^\alpha\big|\big|e^{(\tau-s)\mathcal{A}(s)}x\big|\big|_X^{1-\alpha}d\tau.\end{aligned} \tag{A.9}$$

In (A.9), we have used the fact that $e^{(\tau-s)\mathcal{A}(s)}x\in\mathcal{D}(\mathcal{A})$ for any $x\in X$. Notice that $\mathcal{A}(s)$ generates an analytic semigroup $e^{\cdot\mathcal{A}(s)}$, according to (Appendix A.8) we have the following estimate

$$\big|\big|\mathcal{A}(s)e^{(\tau-s)\mathcal{A}(s)}\big|\big|_X^\alpha\leq C(\tau-s)^{-\alpha}e^{\omega\alpha(\tau-s)}. \tag{A.10}$$

Substituting (A.10) into (A.9), we obtain that,

$$\begin{aligned}&\big|\big|(\mathcal{U}(t,s)-e^{(t-s)\mathcal{A}(s)})x\big|\big|_X\\ \leq&\int_s^t Ce^{\omega(t-\tau)}(\tau-s)^{\beta-\alpha}e^{\omega(\tau-s)}d\tau||x||_X=\frac{C}{1+\beta-\alpha}e^{\omega(t-s)}(t-s)^{1+\beta-\alpha}||x||_X.\end{aligned} \tag{A.11}$$

Thus, we get the estimate for the operator in the norm $||\cdot||_X$

$$\big|\big|\mathcal{U}(t,s)-e^{(t-s)\mathcal{A}(s)}\big|\big|_X\leq\frac{C}{1+\beta-\alpha}e^{\omega(t-s)}(t-s)^{1+\beta-\alpha}. \tag{A.12}$$

We denote $\mathcal{U}(T,0)=\prod_{k=0}^{M-1}\mathcal{U}((k+1)\Delta t,k\Delta t)$. Using the telescoping sum argument, we

obtain

$$\big|\big|\mathcal{U}(T,0)-\prod_{k=0}^{M-1}e^{\Delta t\mathcal{A}(k\Delta t)}\big|\big|_X \tag{A.13}$$

$$=\Big|\Big|\sum_{j=0}^{M-1}\prod_{k=j+1}^{M-1}U((k+1)\Delta t,k\Delta t)\big(\mathcal{U}((j+1)\Delta t,j\Delta t)-e^{\Delta t\mathcal{A}(j\Delta t)}\big)\prod_{l=0}^{j-1}e^{\Delta t\mathcal{A}(l\Delta t)}\Big|\Big|_X \tag{A.14}$$

$$\leq\sum_{j=0}^{M-1}e^{\omega(N-j-1)\Delta t}\frac{C}{1+\beta-\alpha}e^{\omega\Delta t}(\Delta t)^{1+\beta-\alpha}e^{\omega j\Delta t}=\frac{Ce^{\omega T}}{1+\beta-\alpha}(\Delta t)^{\beta-\alpha}. \tag{A.15}$$

The statement in (A.7) is proved. □

For higher order operator splitting methods, in some specific situation the higher order convergence has been proved in [16, 17]. In their works, the assumption Appendix A.7 was largely strengthen, both for the operator $\mathcal{A}(t)$ and initial condition, and the convergence was largely depends on the graph norm $||v||_\alpha := ||\mathcal{A}(t)^\alpha v||_X$. The convergence in norm $||\cdot||_X$ is still open and will be our future reasearch plan.

Appendix A.2. Operator splitting methods for solving non-autonomous evolution equations We study the approximation error of operator splitting methods in solving non-autonomous evolution equations. To be specific, we consider an abstract NCP as follows

$$\begin{cases}\dfrac{d}{dt}u(t)=(\mathcal{A}(t)+\mathcal{B}(t))u(t), \quad t\geq s\in\mathbb{R}\\ \quad u(s)=x\in X\end{cases} \tag{A.16}$$

on a Banach space X, where $\mathcal{A}(t)$ and $\mathcal{B}(t)$ are linear operators, $\mathcal{D}(\mathcal{A}(t))$ is independent of t and dense in X, and for each $t\in\mathbb{R}$, $\mathcal{A}(t)$, $\mathcal{B}(t)$ and $\mathcal{A}(t)+\mathcal{B}(t)$ generate strongly continuous semigroups $e^{\cdot\mathcal{A}(t)}$, $e^{\cdot\mathcal{B}(t)}$ and $e^{\cdot(\mathcal{A}(t)+\mathcal{B}(t))}$, respectively. Furthermore, due to the property of evolution equation, solving $u(t)$ and solving $e^{\gamma_1 t}u(t)$ is equivalent, we assume $\big|\big|e^{\tau\mathcal{A}(t)}\big|\big|_X\leq 1,\big|\big|e^{\tau\mathcal{B}(t)}\big|\big|_X\leq 1,\big|\big|e^{\tau(\mathcal{A}(t)+\mathcal{B}(t))}\big|\big|_X\leq 1$.

We will study the NCP (A.16) based on the perturbation theory. We assume $\mathcal{A}(t)$ is a sectorial operator, which generates an analytical semigroups $e^{\cdot\mathcal{A}(t)}$, and assume $\mathcal{B}(t)$ is bounded, thus $\mathcal{A}(t)+\mathcal{B}(t)$ is also sectorial and generates an analytical semigroups $e^{\cdot(\mathcal{A}(t)+\mathcal{B}(t))}$, where $\mathcal{D}(\mathcal{A}(t)+\mathcal{B}(t))=\mathcal{D}(\mathcal{A}(t))$. In addition, we assume that the operator $\mathcal{A}(t)+\mathcal{B}(t)$ satisfies assumptions Appendix A.6 and Appendix A.7. Therefore, the corresponding evolution family $\mathcal{U}(t,s)$ solves the NCP problem $A.16$ and admits an Euler-type approximation, i.e.,

$$\big|\big|\mathcal{U}(T,0)-\prod_{k=0}^{M-1}e^{\Delta t(\mathcal{A}+\mathcal{B})(k\Delta t)}\big|\big|_X\leq C(T)(\Delta t)^{\beta-\alpha}, \tag{A.17}$$

where $T=M\Delta t$, α,β are constants defined in assumptions Appendix A.6 and Appendix A.7.

In the sequel, we analyze the error between $\prod_{k=0}^{M-1}e^{\Delta t(\mathcal{A}+\mathcal{B})(k\Delta t)}$ and $\prod_{k=0}^{M-1}e^{\Delta t\mathcal{A}(k\Delta t)}e^{\Delta t\mathcal{B}(k\Delta t)}$.

First, we list all the assumptions as follows:

Assumption Appendix A.10. 1. $\mathcal{A}(t)_{t\geq 0}$ and $\mathcal{B}(t)_{t\geq 0}$ are all linear operators (may be unbounded) on X,

2. $\mathcal{D}(\mathcal{A}(t))$ are the same for all t and dense in X,
3. $||\mathcal{B}(t)||_X < C$ for all $t \geq 0$,
4. $\mathcal{A}(t)$ satisfies Appendix A.6 and $\mathcal{A}(t) + \mathcal{B}(t)$ satisfies Appendix A.6 and Appendix A.7,
5. $||e^{\tau\mathcal{A}(t)}||_X \leq 1$,$||e^{\tau\mathcal{B}(t)}||_X \leq 1$,$||e^{\tau(\mathcal{A}(t)+\mathcal{B}(t))}||_X \leq 1$ for all $\tau \geq 0$.

To obtain a convergence theorem, we need an extra assumption in $\mathcal{A}$ and $\mathcal{B}$:

Assumption Appendix A.11. For the commutator $[\mathcal{A}(t), \mathcal{B}(t)] = \mathcal{A}(t)\mathcal{B}(t) - \mathcal{B}(t)\mathcal{A}(t)$, we assume that there is a non-negative γ with

$$\big|\big|[\mathcal{A}(t), \mathcal{B}(t)]x\big|\big|_X \leq c_1\big|\big|\mathcal{A}(t)x\big|\big|_X^{\gamma}||x||_X^{1-\gamma},\ \forall\ x \in \mathcal{D}(\mathcal{A}). \tag{A.18}$$

Next is a standard result from [18], and we prove it here.

Theorem Appendix A.12. Suppose assumptions Appendix A.10 and Appendix A.11 are satisfied. We have the following error estimate for the operator splitting method,

$$\big|\big|(e^{\tau\mathcal{A}(t)}e^{\tau\mathcal{B}(t)} - e^{\tau(\mathcal{A}(t)+\mathcal{B}(t))})x\big|\big|_X \leq C_1\tau^{2-\gamma}||x||_X,\ \forall x \in X, \tag{A.19}$$

where C_1 depends only on c_1, γ and $||\mathcal{B}||_X$.

Proof. We use the freezing coefficient formula and obtain

$$e^{\tau(\mathcal{A}(t)+\mathcal{B}(t))}x = e^{\tau(\mathcal{A}(t))}x + \int_0^{\tau} e^{s\mathcal{A}(t)}\mathcal{B}(t)e^{(\tau-s)(\mathcal{A}(t)+\mathcal{B}(t))}xds. \tag{A.20}$$

Expressing the term $e^{(\tau-s)(\mathcal{A}(t)+\mathcal{B}(t))}$ using the integral form (A.20), we have

$$e^{\tau(\mathcal{A}(t)+\mathcal{B}(t))}x = e^{\tau(\mathcal{A}(t))}x + \int_0^{\tau} e^{s\mathcal{A}(t)}\mathcal{B}(t)e^{(\tau-s)\mathcal{A}(t)}xds + R_1x, \tag{A.21}$$

where

$$R_1 = \int_0^{\tau} e^{s\mathcal{A}(t)}\mathcal{B}(t)\int_0^{\tau-s} e^{\sigma\mathcal{A}(t)}\mathcal{B}(t)e^{(\tau-s-\sigma)(\mathcal{A}(t)+\mathcal{B}(t))}d\sigma ds. \tag{A.22}$$

We can easily verify that the term R_1 is bounded, i.e., $||R_1||_X \leq \frac{1}{2}\tau^2||\mathcal{B}(t)||_X^2$.

On the other hand side, we express the term $e^{\tau\mathcal{B}(t)}$ into exponential series and obtain

$$e^{\tau\mathcal{A}(t)}e^{\tau\mathcal{B}(t)}x = e^{\tau\mathcal{A}(t)}x + \tau e^{\tau\mathcal{A}(t)}\mathcal{B}(t)x + R_2x, \tag{A.23}$$

where $||R_2||_X \leq \frac{1}{2}\tau^2||\mathcal{B}(t)||_X^2$.

Denoted by $f(s) = e^{s\mathcal{A}(t)}\mathcal{B}(t)e^{(\tau-s)\mathcal{A}(t)}x$, we have

$$e^{\tau\mathcal{A}(t)}e^{\tau\mathcal{B}(t)}x - e^{\tau(\mathcal{A}(t)+\mathcal{B}(t))}x = \tau f(\tau) - \int_0^{\tau} f(s)ds + r = d + r, \tag{A.24}$$

where $d = \tau f(\tau) - \int_0^\tau f(s)ds = \tau^2 \int_0^1 \theta f'(\theta\tau)d\theta$ and $r = R_2 x - R_1 x$.

Since $f'(s) = e^{s\mathcal{A}(t)}[\mathcal{A}(t), \mathcal{B}(t)]e^{(\tau-s)\mathcal{A}(t)}x$, assumption Appendix A.11 implies

$$\big|\big|e^{s\mathcal{A}(t)}[\mathcal{A}(t), \mathcal{B}(t)]e^{(\tau-s)\mathcal{A}(t)}x\big|\big|_X \leq c_1||e^{s\mathcal{A}(t)}||_X||\mathcal{A}(t)e^{(\tau-s)\mathcal{A}(t)}x\big|\big|_X^\gamma \big|\big|e^{(\tau-s)\mathcal{A}(t)}x\big|\big|_X^{1-\gamma}. \quad (A.25)$$

By using the property of analytic semigroup Appendix A.8, we know that

$$\big|\big|\mathcal{A}(t)e^{(\tau-s)\mathcal{A}(t)}x\big|\big|_X \leq C(\tau - s)^{-1}||x||_X. \quad (A.26)$$

Thus, we have

$$\begin{aligned} ||d||_X = \big|\big|\tau^2 \int_0^1 \theta f'(\theta\tau)d\theta\big|\big|_X \leq & |\tau^2 \int_0^1 C\theta(\tau - \theta\tau)^{-\gamma}d\theta|||v||_X \\ = & \frac{C}{(1-\gamma)(2-\gamma)}\tau^{2-\gamma}||v||_X. \end{aligned} \quad (A.27)$$

Notice that $||r||_X \leq \tau^2||\mathcal{B}||_X^2$. We finish the proof. □

Using the one step estimate obtained in Theorem Appendix A.12, we finally obtain the error estimate for the operator splitting method.

Theorem Appendix A.13. Suppose assumptions Appendix A.10 and Appendix A.11 hold ture. We have the following error estimate for the operator splitting method in solving the NCP (A.16).

$$||\prod_{k=0}^{N-1} e^{\Delta t(\mathcal{A}+\mathcal{B})(k\Delta t)} - \prod_{k=0}^{N-1} e^{h\mathcal{A}(k\Delta t)}e^{\Delta t\mathcal{B}(k\Delta t)}\big|\big|_X \leq C_1(\Delta t)^{1-\gamma}, \quad (A.28)$$

where C_1 is a constant independent of γ.

Proof. We take $t = j\Delta t$ and $s = (j-1)\Delta t$ for $j = 1, \cdots, M-1$ in Theorem Appendix A.12, and by using the telescoping sum argument, we obtain that for any $x \in X$,

$$\begin{aligned} & ||\prod_{k=0}^{M-1} e^{\Delta t(\mathcal{A}+\mathcal{B})(k\Delta t)}x - \prod_{k=0}^{M-1} e^{\Delta t\mathcal{A}(k\Delta t)}e^{\Delta t\mathcal{B}(k\Delta t)}x\big|\big|_X \\ = & \Big|\Big|\sum_{j=0}^{M-1}\prod_{k=j+1}^{M-1} e^{\Delta t(\mathcal{A}+\mathcal{B})(k\Delta t)}\big(e^{\Delta t(\mathcal{A}+\mathcal{B})(j\Delta t)} - e^{\Delta t\mathcal{A}(j\Delta t)}e^{\Delta t\mathcal{B}(j\Delta t)}\big)\prod_{l=0}^{j-1} e^{\Delta t\mathcal{A}(l\Delta t)}e^{\Delta t\mathcal{B}(l\Delta t)}x\Big|\Big|_X \\ \leq & \sum_{j=0}^{M-1} C_1(\Delta t)^{2-\gamma}\big|\big|\prod_{l=0}^{j-1} e^{\Delta t\mathcal{A}(l\Delta t)}e^{\Delta t\mathcal{B}(l\Delta t)}x\big|\big|_X \leq \sum_{j=0}^{M-1} C_1(\Delta t)^{2-\gamma}||x||_X = C_1(\Delta t)^{1-\gamma}||x||_X. \end{aligned} \quad (A.29)$$

Thus, we finish the proof. □

References

[1] A. Bátkai, P. Csomós, B. Farkas, and G. Nickel, *Operator splitting for non-autonomous evolution equations*, Journal of Functional Analysis, 260 (2011), pp. 2163–2190.

[2] H. Berestycki, F. Hamel, and N. Nadirashvili, *The speed of propagation for KPP type problems. I: Periodic framework*, Journal of The European Mathematical Society, 7 (2005), pp. 173–213.

[3] N. Brummell, F. Cattaneo, and S. Tobias, *Linear and nonlinear dynamo properties of time-dependent ABC flows*, Fluid Dynamics Research, 28 (2001), p. 237.

[4] C. Chicone and Y. Latushkin, *Evolution semigroups in dynamical systems and differential equations*, no. 70, American Mathematical Soc., 1999.

[5] S. Childress and A. D. Gilbert, *Stretch, twist, fold: the fast dynamo*, vol. 37, Springer Science & Business Media, 1995.

[6] P. Del Moral, *Feynman-kac formulae*, in Feynman-Kac Formulae, Springer, 2004, pp. 47–93.

[7] F. Den Hollander, *Large deviations*, vol. 14, American Mathematical Soc., 2008.

[8] T. Dombre, U. Frisch, J. M. Greene, M. Henon, A. Mehr, and M. Soward, *Chaotic streamlines in the ABC flows*, J. Fluid Mech., 167 (1986), pp. 353–391.

[9] K. Engel and R. Nagel, *One-parameter semigroups for linear evolution equations*, vol. 194, Springer Science & Business Media, 1999.

[10] G. Ferré and G. Stoltz, *Error estimates on ergodic properties of discretized Feynman–Kac semigroups*, Numerische Mathematik, 143 (2019), pp. 261–313.

[11] R. Fisher, *The wave of advance of advantageous genes*, Annals of eugenics, 7 (1937), pp. 355–369.

[12] W. Foulkes, L. Mitas, R. Needs, and G. Rajagopal, *Quantum monte carlo simulations of solids*, Reviews of Modern Physics, 73 (2001), p. 33.

[13] D. Galloway and M. Proctor, *Numerical calculations of fast dynamos in smooth velocity fields with realistic diffusion*, Nature, 356 (1992), p. 691.

[14] J. Gärtner and M. Freidlin, *On the propagation of concentration waves in periodic and random media*, in Doklady Akademii Nauk, vol. 249, Russian Academy of Sciences, 1979, pp. 521–525.

[15] P. Hess, *Periodic-parabolic boundary value problems and positivity*, Longman, 1991.

[16] M. Hochbruck and C. Lubich, *On Magnus integrators for time-dependent Schrödinger equations*, SIAM Journal on Numerical Analysis, 41 (2003), pp. 945–963.

[17] M. Hochbruck and A. Ostermann, *Exponential integrators*, Acta Numerica, 19 (2010), pp. 209–286.

[18] T. Jahnke and C. Lubich, *Error bounds for exponential operator splittings*, BIT Numerical Mathematics, 40 (2000), pp. 735–744.

[19] T. Kato, *Perturbation theory for linear operators*, vol. 132, Springer Science & Business Media, 2013.

[20] A. Kolmogorov, I. Petrovsky, and N. Piskunov, *Investigation of the equation of diffusion combined with increasing of the substance and its application to a biology problem*, Bull. Moscow State Univ. Ser. A: Math. Mech, 1 (1937), pp. 1–25.

[21] J. Lyu, Z. Wang, J. Xin, and Z. Zhang, *Convergence analysis of stochastic structure-preserving schemes for computing effective diffusivity in random flows*, SIAM Journal on Numerical Analysis, 58 (2020), pp. 3040–3067.

[22] A. Majda and P. Souganidis, *Large scale front dynamics for turbulent reaction-diffusion equations with separated velocity scales*, Nonlinearity, 7 (1994), p. 1.

[23] S. Meyn and R. L. Tweedie, *Stochastic Stability of Markov Chains*, Springer, New York, 1992.

[24] G. Milstein, J. G., and V. S., *Transition density estimation for stochastic differential equations via forward-reverse representations*, Bernoulli, 10, pp. 281–312.

[25] P. D. Moral and A. Guionnet, *On the stability of interacting processes with applications to filtering and genetic algorithms*, Annales De L Institut Henri Poincare-probabilites Et Statistiques, 37 (2001), pp. 155–194.

[26] P. D. Moral and L. Miclo, *Branching and interacting particle systems approximations of Feynman-Kac formulae with applications to non-linear filtering*, in Seminaire de probabilites XXXIV, Springer, 2000, pp. 1–145.

[27] J. Nolen, J. Roquejoffre, L. Ryzhik, and A. Zlatoš, *Existence and non-existence of Fisher-KPP transition fronts*, Archive for Rational Mechanics and Analysis, 203 (2012), pp. 217–246.

[28] J. Nolen, M. Rudd, and J. Xin, *Existence of KPP fronts in spatially-temporally periodic advection and variational principle for propagation speeds*, Dynamics of PDEs, 2 (2005), pp. 1–24.

[29] J. Nolen and J. Xin, *Computing reactive front speeds in random flows by variational principle*, Physica D: Nonlinear Phenomena, 237 (2008), pp. 3172–3177.

[30] ——, *Asymptotic spreading of KPP reactive fronts in incompressible space-time random flows*, Ann Inst. H. Poincare, Analyse Non Lineaire, 26 (2009), pp. 815–839.

[31] A. Pazy, *Semigroups of linear operators and applications to partial differential equations*, vol. 44, Springer Science & Business Media, 2012.

[32] L. Ryzhik and A. Zlatoš, *KPP pulsating front speed-up by flows*, Communications in Mathematical Sciences, 5 (2007), pp. 575–593.

[33] R. Schnaubelt, *Well-posedness and asymptotic behaviour of non-autonomous linear evolution equations*, in Evolution equations, semigroups and functional analysis, Springer, 2002, pp. 311–338.

[34] J. Shen, T. Tang, and L. Wang, *Spectral methods: algorithms, analysis and applications*, vol. 41, Springer Science & Business Media, 2011.

[35] L. Shen, J. Xin, and A. Zhou, *Finite element computation of KPP front speeds in 3D cellular and ABC flows*, Mathematical Modelling of Natural Phenomena, 8 (2013), pp. 182–197.

[36] ——, *Finite element computation of KPP front speeds in cellular and cat's eye flows*, Journal of Scientific Computing, 55 (2013), pp. 455–470.

[37] H. Stewart, *Generation of analytic semigroups by strongly elliptic operators*, Transactions of the American Mathematical Society, 199 (1974), pp. 141–162.

[38] Z. Wang, J. Xin, and Z. Zhang, *Convergence analysis of a lagrangian scheme in computing effective diffusivity of 3D time-dependent flows*. In preparation.

[39] ——, *Sharp uniform in time error estimate on a stochastic structure-preserving Lagrangian method and computation of effective diffusivity in 3D chaotic flows*. To appear in SIAM Multiscale Model. Simul., arXiv:1808.06309.

[40] ——, *Computing effective diffusivity of chaotic and stochastic flows using structure-preserving schemes*, SIAM Journal on Numerical Analysis, 56 (2018), pp. 2322–2344.

[41] J. Xin, *An introduction to fronts in random media*, vol. 5, Springer Science & Business Media, 2009.

[42] P. Zu, L. Chen, and J. Xin, *A computational study of residual KPP front speeds in time-periodic cellular flows in the small diffusion limit*, Physica D: Nonlinear Phenomena, 311 (2015), pp. 37–44.